ELSEVIER

Cretaceous Research 26 (2005) 699–725

CRETACEOUS RESEARCH

www.elsevier.com/locate/CretRes

Stratigraphy and palaeoenvironment of the dinosaur-bearing Upper Cretaceous Iren Dabasu Formation, Inner Mongolia, People's Republic of China

Jimmy Van Itterbeeck [a,*], David J. Horne [b], Pierre Bultynck [a,c], Noël Vandenberghe [a]

[a] *Afdeling Historische Geologie, Laboratorium voor Stratografie, Katholieke Universiteit Leuven, Redingenstraat 16, B-3000 Leuven, Belgium*
[b] *Department of Geography, Queen Mary, University of London, Mile End Road, London E1 4NS, UK and Department of Zoology, The Natural History Museum, Cromwell Road, London SW7 5BD, UK*
[c] *Departement Paleontologie, Koninklijk Belgisch Instituut voor Natuurwetenschappen, Vautierstraat 29, B-1000 Brussel, Belgium*

Received 26 March 2004; accepted in revised form 24 March 2005
Available online 9 September 2005

Abstract

New field observations and sedimentological analyses of the dinosaur-bearing Upper Cretaceous Iren Dabasu Formation in the Iren Nor region of Inner Mongolia (People's Republic of China) have led to a better understanding of its palaeoenvironment. The fluvial deposits represent a braided river that, due to the large amount of fines, does not fit the classical model for braided rivers. The study area is divided into two parts: in the northern part, sediments of the main channel belt of the ancient braided river system are exposed along a dry river valley on the northern edge of the Iren Nor salt lake, while in the southern part, comprising all other studied exposures, different facies of the ancient floodplain are represented, including minor channels, temporary ponds, and palaeosols. The difference between the northern and southern parts is also reflected in the fossil content; only the southern exposures have yielded dinosaur remains. The ancient braided river had a broad, vegetated floodplain populated by a diverse dinosaur fauna. Four species of charophytes are described and illustrated from the Iren Nor site, together with eight species of ostracods, one of which (*Cyprídea irennorensis* sp. nov.) is new. Contrary to the vertebrate data, both groups of microfossils indicate a latest Cretaceous age (Campanian–Maastrichtian) for the Iren Dabasu Formation, and suggest a possible correlation with the Nemegt Formation, which would allow the age estimation to be refined to latest Campanian–Early Maastrichtian.

Keywords: Inner Mongolia; Iren Dabasu Formation; Late Cretaceous; Charophyta; Ostracoda

1. Introduction

The Sino-Belgian Dinosaur Expedition (SBDE, 1995–2002), a collaboration between the Inner Mongolia Museum, Hohhot and the Royal Belgian Institute of Natural Sciences, Brussels, aimed to elucidate the replacement of Early Cretaceous iguanodontids by Late Cretaceous hadrosaurids. Accordingly, the SBDE has conducted three field campaigns on the Iren Dabasu Formation at the Iren Nor site in the vicinity of Erenhot (Fig. 1) to collect more material of the primitive Hadrosauroidea *Bactrosaurus johnsoni* and *Gilmoreosaurus mongoliensis*.

The first dinosaur discoveries at the Iren Nor site, the first known dinosaur locality in Central Asia, were made in 1922 during the Central Asiatic Expeditions of the American Museum of Natural History. Since then, numerous expeditions have visited the area and

* Corresponding author.
E-mail address: jimmy.vanitterbeeck@geo.kuleuven.be (J. Van Itterbeeck).

0195-6671/$ - see front matter © 2005 Elsevier Ltd. All rights reserved.
doi:10.1016/j.cretres.2005.03.004

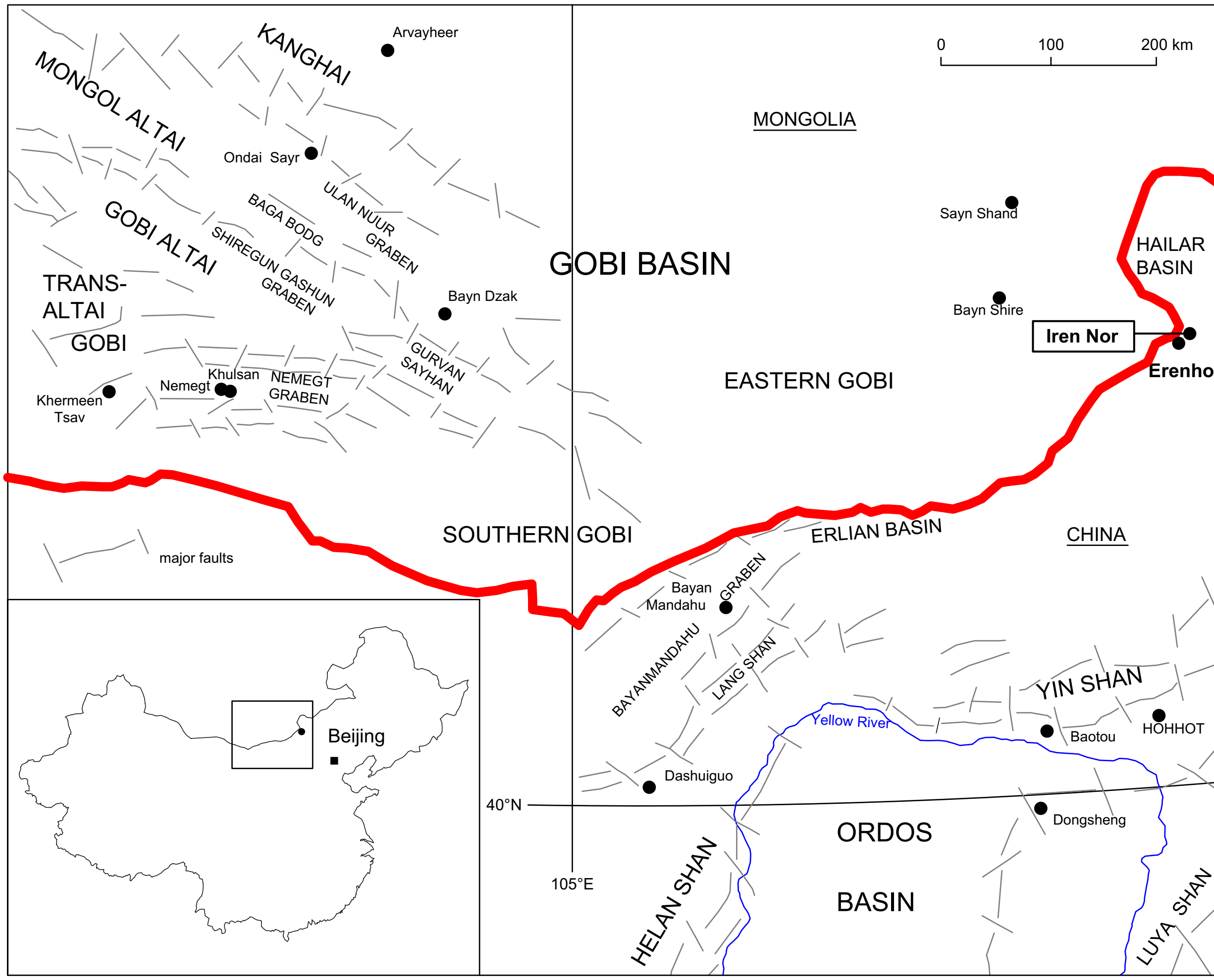

Fig. 1. Generalised map of the Gobi Basins, showing the location of Erenhot and Iren Nor (modified after Jerzykiewicz, 1995). Inset shows the general location of the area within the P.R. China.

extracted dinosaur fossils (see Currie and Eberth, 1993 for an overview). In spite of this long tradition of palaeontological expeditions, however, it was not until the Sino-Canadian expedition in the early 1990s that studies of the sedimentology and palaeoecology of the site were initiated (Currie and Eberth, 1993). During the different SBDE field campaigns, sedimentological, stratigraphical and palaeontological data were gathered to complement the earlier work. Here we present the results of these studies, including the first list of micropalaeontological taxa, thus facilitating a more detailed interpretation of the palaeoecology of the Iren Nor site and providing an opportunity for discussion of the age of the Iren Dabasu Formation.

2. Stratigraphical and geological setting

The China-Mongolia border region contains many Late Mesozoic extensional basins, including the Chinese Erlian and the Mongolian Gobi Basins (Meng et al., 2003). The latter is sometimes divided into smaller basins (e.g., Graham et al., 2001). These extensional basins consist of a series of subbasins separated by intrabasinal highs, and all have a similar tectonic history (Meng et al., 2003). Two regional unconformities divide the sedimentary record into three megasequences: prerift, synrift and postrift deposits (Graham et al., 2001). The Late Jurassic and Early Cretaceous synrift sediments are relatively thick and contain abundant volcanic intercalations, while the Upper Cretaceous postrift strata are relatively thin and devoid of volcanics (Shuvalov, 2000).

The Iren Nor site is situated in the Erlian Basin but it has often been compared to the Mongolian dinosaur sites of the Gobi Basin. Therefore, a short review of the Upper Cretaceous stratigraphy of the Gobi Basin is provided, followed by an overview of the geological setting of the Iren Nor site and previous estimations of the stratigraphical position and age of the Iren Dabasu Formation.

2.1. The Gobi Basin

Due to repeated intervals of block faulting, the sedimentary sequences are discontinuous and contain several hiatuses and unconformities; nowhere in the Gobi Basin is a complete stratigraphical column preserved, but composite sections have been compiled (Jerzykiewicz and Russell, 1991; Shuvalov, 2000). Unfortunately there are no standard rules for the correct transcription of the Mongolian names, so that a large variety of different names is used: Hühteeg and Bayanshiree (Shuvalov, 2000) are the equivalents of, respectively, Khukhtek and Bayn Shire (Jerzykiewicz and Russell, 1991). Another and more important complication is the different stratigraphical concepts used by different workers. Russian and Mongolian scientists use "svita" as the fundamental stratigraphic unit, combining both lithostratigraphical and chronostratigraphical concepts; the boundaries of a svita are considered to be isochronous. European and American scientists, on the other hand, use 'formations' to group rocks, clearly a lithostratigraphical concept without time implications. Care must therefore be taken when comparing svitas and formations (Barsbold, 1972; Gradzinski et al., 1977; Hicks et al., 1999).

All the Mesozoic deposits in the Gobi Basin are entirely terrestrial/continental, since the last major marine incursion in Central Asia occurred during the Permian. The lack of marine fossils precludes direct biostratigraphical correlation of the deposits with international marine stages. As a consequence, non-marine fossils have been used to correlate the lithostratigraphical units of the Gobi Basin with the international standard scale, by reference to sections containing interdigitations of marine and terrestrial fossils, either in Asia or North America. Ages of the Lower Cretaceous formations of the Gobi were estimated largely on the basis of plant megafossils (Krassilov, 1982) and molluscs (Martinson and Kolesnikov, 1974; Martinson, 1982). Ages of the Upper Cretaceous formations of the Gobi are based on comparisons of the vertebrates with those of North American non-marine units, which are constrained by ammonite and palynological biozonations and calibrated by chronostratigraphical methods (Gradzinski et al., 1977; Fox, 1978; Lillegraven and McKenna, 1986; Jerzykiewicz and Russell, 1991). Such correlations are severely hampered by the endemic nature of the Cretaceous vertebrate assemblages in the Gobi. A few attempts have been made to correlate the Cretaceous of the Gobi directly with the international standard scale by using radiometric ages of intercalated volcanic deposits (Shuvalov, 2000 and references therein) and palaeomagnetic analyses (Hicks et al., 1999).

There is a general consensus that the Upper Cretaceous deposits of the Gobi can be divided into four formations: the Nemegt, Barun Goyot, Djadokhta and Bayn Shire formations. The Nemegt and Barun Goyot formations have been defined by Gradzinski and Jerzykiewicz (1974) and formally described by Gradzinski et al. (1977). Based on the presence of the hadrosaurine dinosaur *Saurolophus*, the Nemegt Formation is correlated with the Early Maastrichtian Edmontonian Stage in North America (Jerzykiewicz and Russell, 1991). The mid-Campanian in North America is characterised by an increase in aridity and a marked change of dinosaur fauna. According to Jerzykiewicz and Russell (1991), this change can also be observed at the boundary between the Bayn Shire and Djadokhta formations. Based on this hypothesis, the Djadokhta and Barun Goyot formations are considered the equivalents of the Judithian Stage of North America, in which case they are respectively mid- and Late Campanian in age. This age estimation is supported by the radiometric ages of the volcanic layers within the Barun Goyot Formation (Fig. 2). The type locality of the Djadokhta Formation (defined by Berkey and Morris, 1927 and redefined by Gradzinski et al., 1977) is situated at the Bayn Dzak locality in Mongolia (Fig. 1), although a more complete and better-studied section is known from the Bayan Mandahu locality in China (Eberth, 1993; Jerzykiewicz et al., 1993).

The Bayn Shire Formation (defined by Vasiliev et al., 1959) is more difficult to date. The freshwater molluscs can be compared with similar species in Cretaceous deposits, interbedded with Cenomanian–Santonian marine strata in the Fergana and Aral Sea regions (Martinson and Kolesnikov, 1974; Makulekov and Kurzanov, 1986). Within the Bayn Shire Formation, a turtle assemblage with *Kizylkumemys shuwalovi* is replaced by one with *Lindholmemys martinsoni*. In former Soviet mid-Asia, this transition, interdigitated with marine sediments, marks the passage from Early to Late Turonian (Nessov, 1984). Based on the molluscan and turtle evidence and the age of the overlying Djadokhta Formation, Jerzykiewicz and Russell (1991) have estimated the age of the Bayn Shire Formation to be Late Turonian–Early Campanian. The palaeomagnetic measurements of Hicks et al. (1999), however, limit the age of the Bayn Shire to the C34 long normal interval, constraining the Bayn Shire to be no older than 83.5 Ma. According to Shuvalov (2000), the Bayn Shire Formation ranges from Cenomanian to Santonian, although the radiometric measurements, given by the same author, indicate a slightly older age, from 101 to 90 Ma (Fig. 2).

2.2. The Iren Dabasu Formation and the Iren Nor dinosaur site

The Iren Dabasu Formation (named by Granger and Berkey, 1922 and formally defined by Berkey and

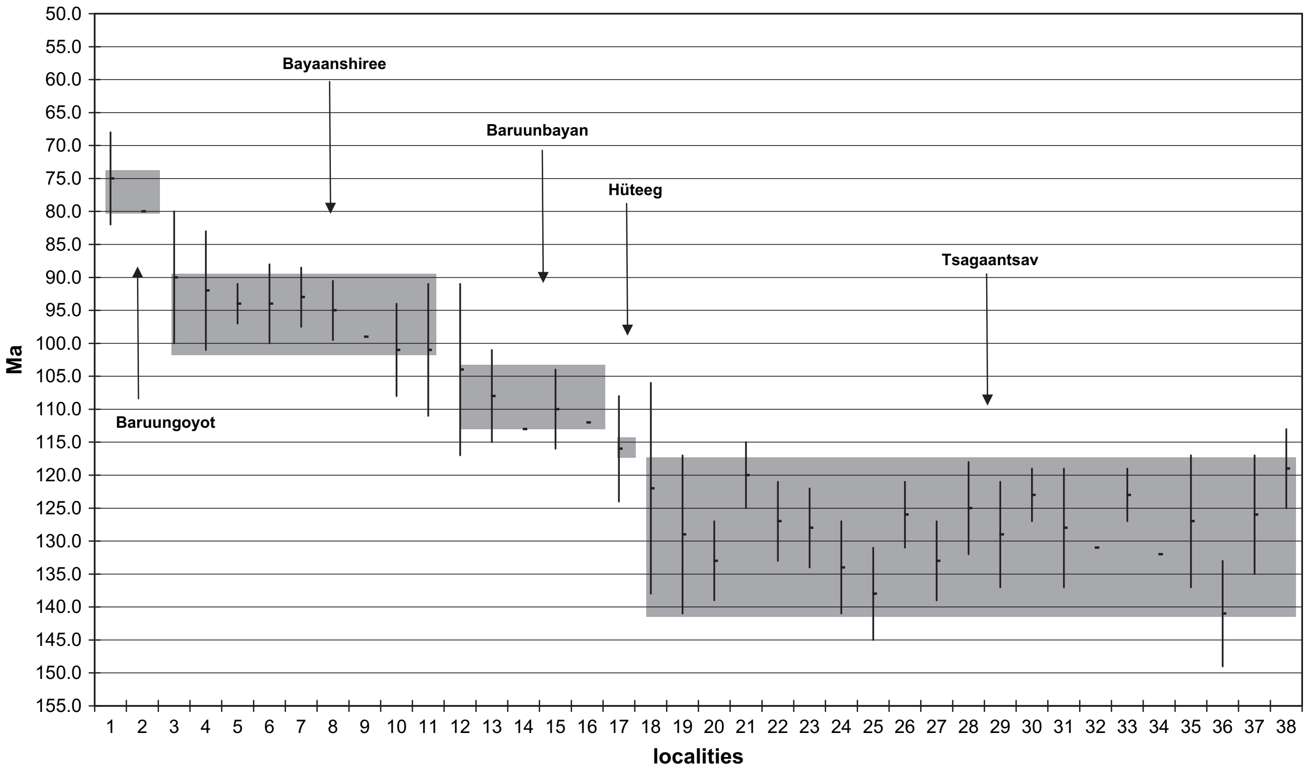

Fig. 2. Radiometric ages of the different Upper Cretaceous suites of the Gobi regions (based on data from Shuvalov, 2000). Numbers on horizontal axis refer to different localities in the Gobi Basin (see Shuvalov, 2000, pp. 261–262, table 14.2).

Morris, 1927, pp. 203–204) crops out around the Iren Nor salt lake (Fig. 3), 8 km northeast of Erenhot. Good exposures are rather rare and limited to low-relief ridges and the channels of a few ephemeral rivers.

According to the description of Berkey and Morris (1927), the formation unconformably overlies Late Proterozoic or Palaeozoic slates on a horizontal contact. As such, the total thickness of the formation would equal the exposed thickness, which measures 30 m (Berkey and Morris, 1927). According to the Bureau of Geology and Mineral Resources of the Nei Mongol Autonomous Region (1991), the slates belong to the Carboniferous. Based on the abrupt lateral change to the north, Currie and Eberth (1993) proposed an E–W normal fault, or system of faults, with the slates on the up-thrown side. This hypothesis is confirmed by new observations along the dry river valley (ERHVAL on Fig. 3) on the northern side of the lake. In the northernmost part of the section, along the river valley (Fig. 4), the Carboniferous outcrops are topographically higher than the Cretaceous and Tertiary sediments; a flat-lying contact, as proposed by Berkey and Morris (1927), can therefore be excluded. The fault plane could not be observed due to the lack of exposures, so exact data on the orientation and throw are lacking. The location of the fault was recognised by the distinct change in colour of the weathered layer covering the sediments. Although the exact total thickness of the formation is unknown, estimations now range from >83 m, on the regional geological map, to 114 m (Bureau of Geology and Mineral Resources of the Nei Mongol Autonomous Region, 1991).

South of the lake, the Iren Dabasu Formation is unconformably overlain by the Eocene Arshanto Formation (Table 1) that crops out in the higher parts of the talus on the southern edge of the lake. The contact is badly exposed; it has been observed at sites T-K and ERH/+ (Fig. 3) as a transition from white to red. The top of the Cretaceous sequence is characterised by the presence of a poorly developed calcrete palaeosol. The development stage of the calcrete shows that a considerable amount of material was eroded before the erosion stopped on a more resistant bed (in this case a calcrete). The red silts at the top are unconformably overlain by yellow, coarse pebbly sands with large-scale cross-stratification belonging to the Oligocene Houldjin Formation. The contact between the two latter formations was observed at the TERT locality (Fig. 3). The Houldjin Formation crops out on the plateau that extends from the lake to the city of Erenhot. North of the lake (ERHVAL), the Iren Dabasu Formation is overlain by red conglomerates belonging to the Eocene Irding Manha Formation.

Berkey and Morris (1927) proposed a Lower Cretaceous age for the Iren Dabasu Formation based on the occurrence of the ornithopod dinosaur *Iguanodon*. More

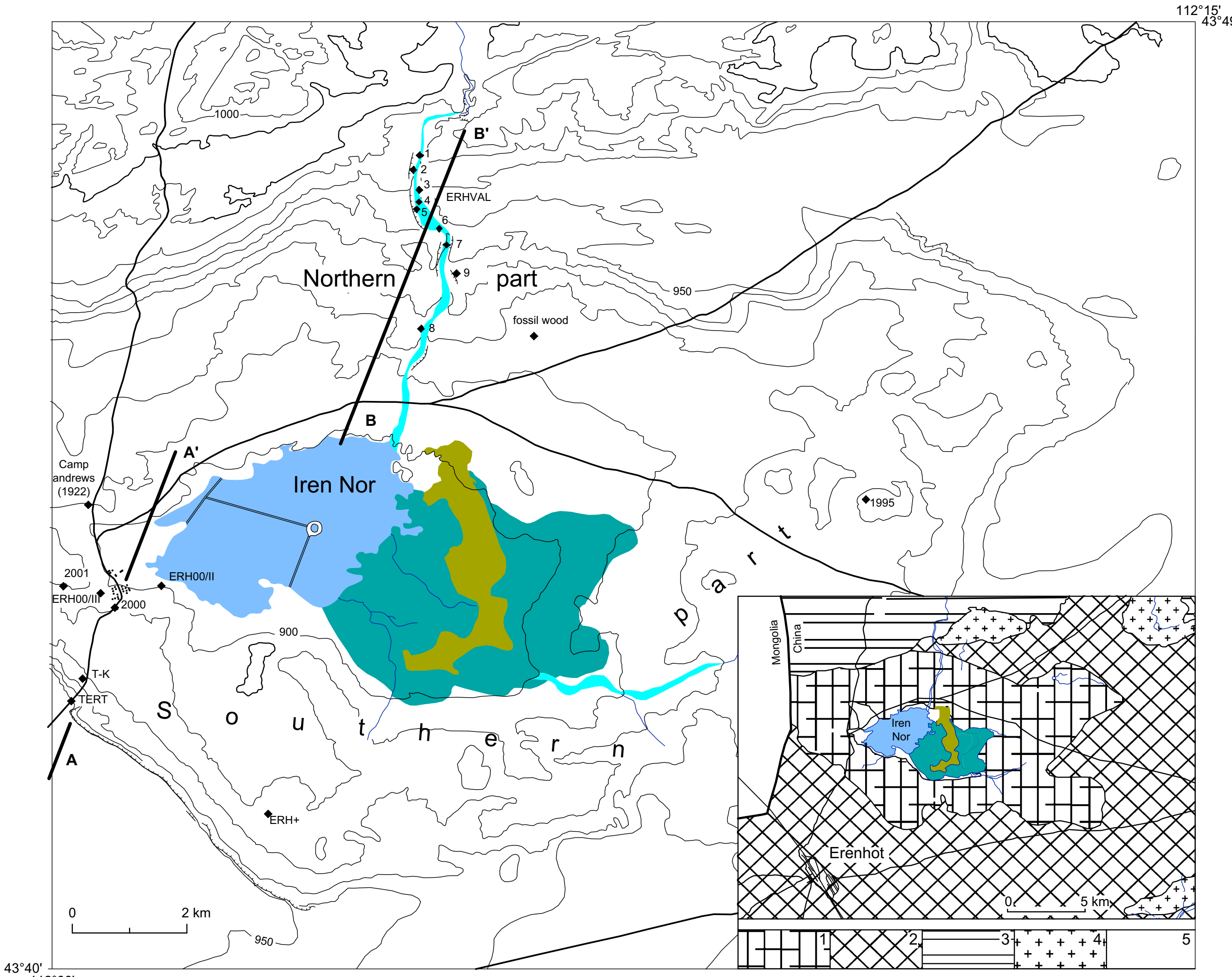

Fig. 3. Simplified topographic map of the Iren Nor area, showing locations of different measured outcrops (shown in Fig. 5) and schematic cross section A-A′ and B-B′ (Fig. 4). The years indicate the location of the major excavation sites of the SBDE: 1995, ERH00/IV; 2000, ERH00/I; 2001, ERH01/V. Inset shows simplified geological map of the area to the northeast of Erenhot; 1, Iren Dabasu Formation; 2, Palaeogene–Neogene; 3, Carboniferous; 4, Plutons; 5, Quaternary.

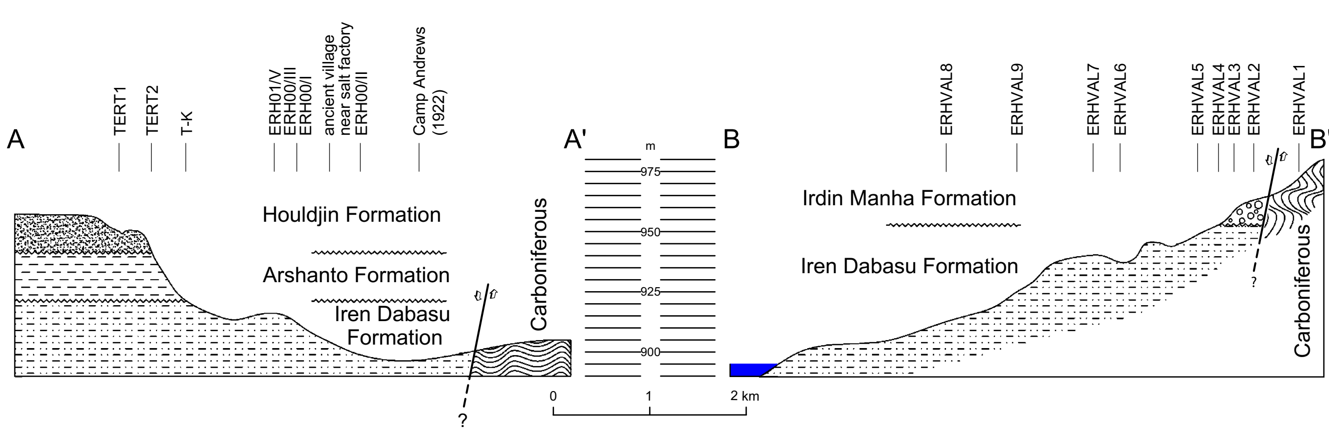

Fig. 4. Schematic cross-sections through the Iren Nor area (see Fig. 3 for exact locations of cross-sections).

Table 1
Overview of the stratigraphy of the Iren Nor region

Formation	Age and thickness		Description
Houldjin	Middle Oligocene	+12m	Yellow pebbly sands and gravel consisting of quartzite, vein quartz, chalcedony, slate and greywacke pebbles
Irding Manha	Middle Eocene	42m	Grey beds of sandy claystones, sandstones and conglomerates, some strata are mottled red and green and a few completely red; characterised by numerous channel-cuts and fillings
Arshanto	Middle Eocene	42m	Red clay- and fine siltstones, septarian nodules present
Iren Dabasu	Upper Cretaceous	114m	Rather coarse, light grey sandstones consisting of angular grains of quartz with minor amounts of chalcedony, quartzite, feldspar, granite and epidote rock, cross-bedded Thinly bedded clay- and siltstones, reddish, buff or slightly yellowish in colour
	Carboniferous		Dark-coloured slates and quartzites

Names and description of formations follow Berkey and Morris (1927); age and thickness after Bureau of Geology and Mineral Resources of the Nei Mongol Autonomous Region (1991).

recently, the age of the formation has been discussed in numerous publications (for an overview, see Table 2) and the age estimations span the entire Late Cretaceous. Three opinions are defended in the literature: firstly, the Iren Dabasu Formation is given as an early Late Cretaceous age (Cenomanian–Turonian) based on the primitive nature of the hadrosaurs (Godefroit et al., 1998 and references therein). Secondly, based on the occurrence of derived theropods (Jerzykiewicz and Russell, 1991; Currie and Eberth, 1993), the age is considered to be mid to late Late Cretaceous (Coniacian–Santonian–?Early Campanian). A third opinion is found in the Chinese literature (Chen, 1983; Liu and Wu, 1990; Ma, 1994) where the Iren Dabasu Formation is dated as late Late Cretaceous (Campanian–Maastrichtian), but this opinion has never been explicitly specified for the sediments at the Iren Nor site.

Jerzykiewicz and Russell (1991) and Currie and Eberth (1993) correlate the Iren Dabasu Formation with the Bayn Shire Formation on the basis of their vertebrate assemblages (Table 3), as previously suggested by Barsbold (1972) based on molluscs. The presence of the non-hadrosaurid hadrosauroid dinosaur *Bactrosaurus johnsoni* in the Bayn Shire Formation (as reported by Tsogbataar, 1997 and mentioned by Hicks et al., 1999), and the presence of the theropod dinosaur *Garudimimus* in the Iren Dabasu Formation (as mentioned by Currie and Eberth, 1993), need to be confirmed in order to support the correlation with the Bayn Shire Formation. Liu (1987) correlated the Iren Dabasu Formation with the Barun Goyot and Nemegt formations on the basis of charophyte evidence.

3. Systematic micropalaeontology

The micropalaeontological content of the dinosaur-bearing sediments has been studied in an attempt to resolve the current debate over the age and correlation of the Iren Dabasu Formation. Using standard methods (Van Itterbeeck et al., 2004, p. 394), over 25 samples were processed for the study of charophytes, ostracods and palynomorphs, as all three microfossil groups have proven their worth in dating continental sediments. Not a single sample yielded fossil palynomorphs and only two samples from the southern part of the lake (Fig. 5) proved rich in ostracods and charophytes; these are described below. The type-specimens of the newly

Table 2
Age estimations of the Iren Dabasu Formation

Reference	Age	Reasoning
Berkey and Morris (1927)	Lower Cretaceous	Presence of iguanodontid fossils
Rozhdestvensky (1966, 1977)	Cenomanian	The primitive character of the hadrosaurid fauna *Bactrosaurus johnsoni* and *Gilmoreosaurus mongoliensis*
Brett-Surman (1979)	pre-Santonian	
Weishampel and Horner (1986)	pre-Turonian	
Godefroit et al. (1998)	early Late Cretaceous	
Jerzykiewicz and Russell (1991)	Late Turonian – Early Campanian	Correlation with the upper part of the Bayn Shire Formation, based on turtle and dinosaur fauna
Currie and Eberth (1993)	Post-Cenomanian, Early Senonian ? Early Campanian	
Li and Liu (1994, fig. 16)	Turonian – Santonian	No reasoning given in the text
Ma (1994, p. 281, Erlian Form.)	Campanian – Maastrichtian	*Pseudohydria-Sainshandia-Limnocyrena* assemblage of bivalves
Liu and Wu (1990, p. 216)	Maastrichtian	No reasoning given in the text
Chen (1983, fig. 5)	Maastrichtian	No reasoning given in the text

Table 3
Correlation of the Iren Dabasu Formation based on the dinosaur, charophyte and ostracod fossils: 1, Weishampel (1990); 2, Currie and Eberth (1993); 3, Tsogbataar (1997); 4, Karczewska and Ziembinska-Tworzydlo (1969, 1981); 5, Kyansep-Romashkina (1980, 1982); 6, present study; 7, Szczechura (1978); 8, Khand (1987); 9, Stankevitch (1982)

species	Nemegt	Barungoyot	Djadokhta	Baynshire	Iren Dabasu
Dinosaurs					
Adasaurus mongoliensis	1				
Alioramus remotus	1				
Anserimimus planinychus	1				
Barsboldia sicinskii	1				
Borogovia gracilicrus	1				
Deinocheirus mirificus	1				
Elismisaurus rarus	1				
Gallimimus bullatus	1				
Gorgosaurus novolijovi	1				
Homalocephale calathocercos	1				
Nemegtosaurus mongoliensis	1				
Opisthocoelicaudia skarzynskii	1				
Oviraptor mongoliensis	1				
Prenocephale prenes	1				
Saurolophus angustirostris	1				
Saurornithoides junior	1				
Tarbosaurus baatar	1				
Tarchia gigantea	1				
Therzinosaurus cheloniformis	1				
Tochisaurus nemegtensis	1				
Ingenia yanshini	1	1			
Velociraptor sp.		1		2	2
Hulsanpes perlei		1			
Conchoraptor gracilis		1			
Saichania chulsanensis		1			
Tarchia kielanae		1			
Bagaceratops rozhdestvenskyi		1			
Breviceratops kozlowskii		1			
Tylocephale gilmorei		1			
Goyocephale lattimorei		1			
Avimimus portentosus		1	1		2 ?
Gallimimus sp.			1		
Oviraptor philoceratops			1		
Pinacosaurus grangeri			1		
Protoceratops andrewsi			1		
Quaesitosaurus orientalis			1		
Saurornithoides mongoliensis			1		2 ?
Tarbosaurus sp.			1		
Velociraptor mongoliensis			1		
Alectrosaurus olseni				1	1
Amtosaurus magnus				1	
Archaeornithomimus asiaticus				2 ?	1
Bactrosaurus johnsoni				3 ?	1
Enigmosaurus mongoliensis				1	
Erlikosaurus andrewsi				1	2 ?
Garudimimus brevipes				1	2 ?
Gilmoreosaurus mongoliensis					1
Segnosaurus galbinensis				1	2 ?
Talarurus plicatospineus				1	2 ?
Charophytes					
Aclistochara cf. bransoni	4				
Amblyochara agathae	4				
Amblyochara nemegtensis	4				
Atopochara ulanensis	4 / 5				6
Grambastichara sp.	4				
Gobichara caerulea	4				
Gobichara viridis	4				
Harrisichara cepaeformis	4				
Harrisichara cretacea	4 / 5			5	
Lamprothamnium altanulanensis	4 / 5				
Lamprothamnium bugintsavica	5				
Latochara sp.	4				
Maedleriella monilifera	4				
Mesochara gradzinskii	4				
Mesochara inflata	4				
Mesochara luculenta	4				
Mesochara mongolica	4 / 5				
Mesochara obventicia	4				
Mesochara orientalis	4				
Mesochara sp.	4				
Mesochara stankevitchii	4 / 5				6
Mesochara texensis	5				
Mesochara voluta	4				
Microchara cf. cristata	4				
?Mongolichara immatura	4				
Mongolichara aurea	4 / 5				
Mongolichara costulata	4 / 5				
Mongolichara fulgida	4				
Mongolichara grovesioides	4				
Mongolichara turnaui	4				
Obtusochara cf. lanpingensis	4				
Obtusochara madleri	4 / 5				
Peckichara praecursoria	4				
Porochara mundula	4				6
Saportanella nana	4 / 5				
Saportanella romaschkinae	4				
Spaerochara jacobii	4				
Sphaerochara verticillata	4 / 5				
Stephanochara castelii	4				
Grambastichara sp.	4 / 5	5			
Maedlerisphaera pseudoulmensis	4 / 5	5			
Mesochara oviformis	5	5			
Mongolichara gobica	4 / 5	5			
Atopochara barungoiotica		5			
Lamprothamnium bambuhudukae		5			
Raskyella rosuliforma		5			
Saportanella barsboldii		5			
Atopochara sp.		5		5	
Mesochara sainshandinica		5		5	
Atopochara restricta				5	
Atopochara aff. trivolvis				5	
Mesochara shuwalovi				5	
Mongolichara attenuata				5	
Mongolichara paucicostata				5	
Nemegtichara prima					6
Ostracods					
Altanicypris bispinifera	7				
Altanicypris multispina	7 / 8 / 9				
Altanicypris nogontsavica	8				
Candona cf. fabaeformis	7				
Candoniella janina	9				
Clinocypris parva	8				
Cypridea barsboldi	7 / 8 / 9				
Cypridea flexodorsalis	9				
Cypridopsis buginstavica	7 / 8 / 9				
Cypris ectypa	7 / 8 / 9				
Eucypris ex gr. gemella	8				
Eucypris toorojensis	8 / 9				6
Eucypris tostiensis	8 / 9				6
Gobiella prima	7				
Leiria alaktsavica	8				
Leiria sp.	7				
Limnocythere sp.	7				
Lycopterocypris cf. profunda	7				
Mediocypris asiatica	8				
Mongolianella ex gr. khamariniensis	9				
Mongolocypris mongolica	8				
Rhinocypris sp.	7				
?Scabriculocypris rasilis	7				
Talicypridea reticulata	7 / 8 / 9				
Timiriasevia cf. miaogouensis	7				
Timiriasevia naranbulakensis	7 / 8 / 9				
Bogdocypris ongoniensis	8	8			
Candona altanulaensis	7 / 8 / 9	8			
Khandia stankevitchae	7 / 8 / 9	9			
Rhinocypris ingenica	7 / 8 / 9	8			
Altanicypris szczechurae	7 / 8 / 9	8 / 8	9		6
Mongolianella cuspidigera	8 / 9	8 / 9	9	9	
Candoniella altanica	7 / 8 / 9	8 / 9	8	8 / 9	
Cypria elata	7 / 9	8 / 9	8	8 / 9	
Cypridea cavernosa	7 / 8 / 9	8 / 9	8 / 9	8 / 9	
Cypridea fracta	8	8	8	8	
Mongolocypris distributa	7 / 8 / 9	8 / 9	8 / 9	8 / 9	6
Timiriasevia minuscula	7 / 8 / 9	8	8	8	
Timiriasevia polymorpha	7 / 8 / 9	8 / 9	8	8 / 9	
Ziziphocypris martinsoni	8	8 / 9	8	8 / 9	
Candona bagmodica	9	9		8	
Cyclocypris transitoria	7 / 8 / 9	9		9	
Eucypris hermintsavica	9	8		9	
Lycopterocypris bajschintsavicus	9	9		8	
Mongolianella ?palmosa	7 / 9	9		9	
Paracypridea mongolica	7 / 9	9		9	
Talicypridea biformata	7 / 9	8 / 9		9	
Talicypridea longiscula	9	9		8 / 9	
Talicypridea obliquecostae	7 / 8 / 9	8 / 9		9	
Ziziphocypris costata	7 / 9	9		8	6
Cypridea halzanensis		8			
Cypridea hongiloensis		8			
Talicypridea abdarantica		8			
Bogdocypris khosbajari		9	8		
Limnocythere barungoiotensis		8 / 9	8 / 9		
Cypridea profusa		8	8	8	
Mongolianella palmosa		8	8	8	
Ilyocypris proteus			8 / 9		
Limnocythere ulannurensis			8 / 9		
Cyprinotus bajandzagensis			8 / 9		
Gobiocypris tugrigensis			9		
Limnocythere bulganensis			8		
Lycopterocypris bagataratchensis			8	8 / 9	
Clinocypris aff. dentiformis				8	
Eucypris khandae				8 / 9	
Eucypris ulantsabica				9	
Mediocypris sp.				8	
Cypridea irennorensis					6
Darwinula sp.					6

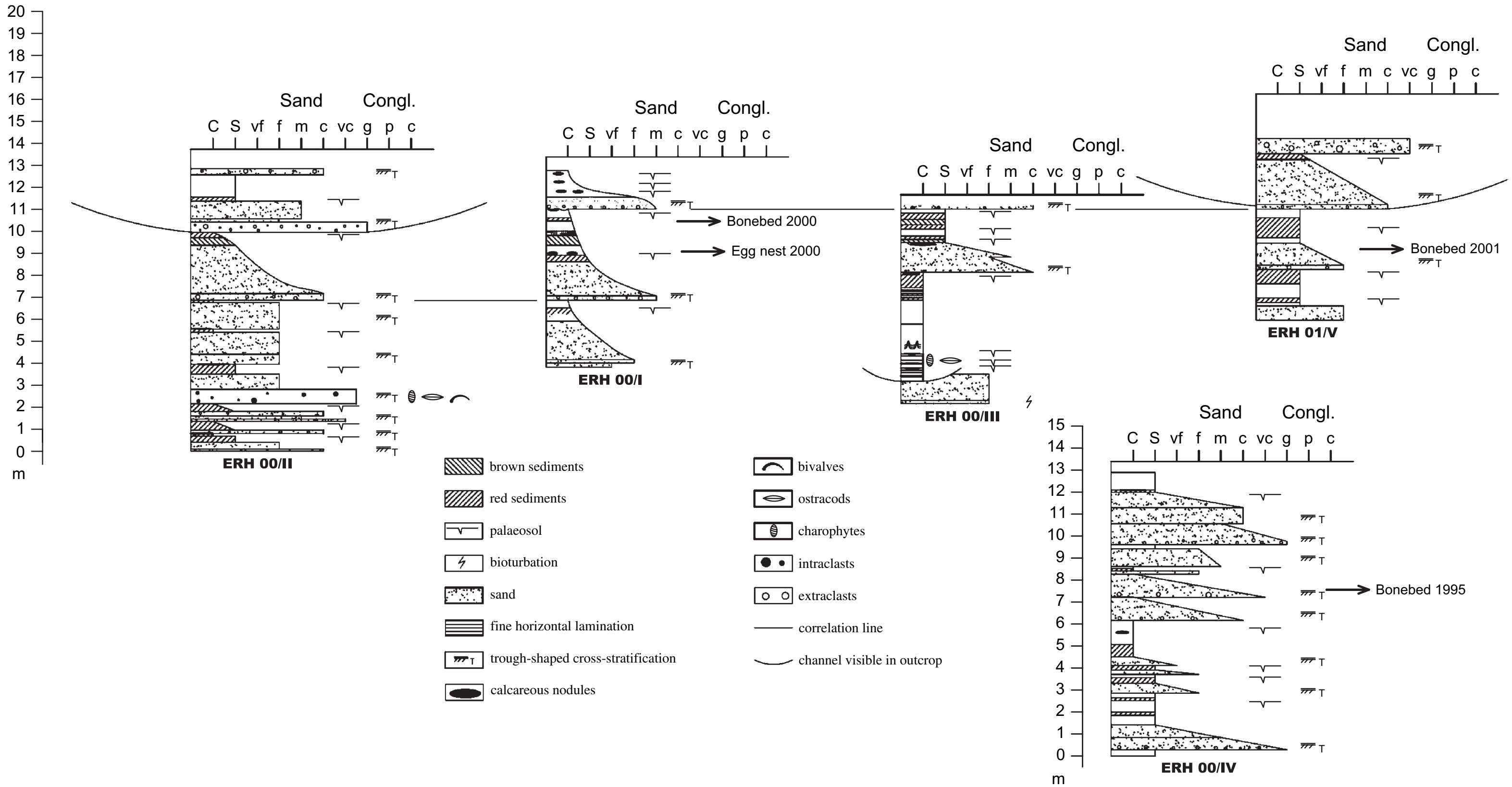

Fig. 5. Lithology of exposures on southern part of Iren Nor salt lake.

described taxa, and all the figured specimens, are deposited in the collections of the Royal Belgian Institute of Natural Sciences (RBINS).

3.1. Ostracods of the Iren Dabasu Formation

Class: Ostracoda Latreille, 1806
Order: Podocopida G.W. Müller, 1894
Suborder: Darwinulocopina Sohn, 1988
Superfamily: Darwinuloidea Brady and Norman, 1889
Family: Darwinulidae Brady and Norman, 1889
Genus *Darwinula* Brady and Robertson in Jones, 1885

Darwinula sp.
Fig. 6M

Material. Two complete carapaces.

Measurements. Length 0.65 mm, height 0.30 mm.

Remarks. Based on the general outline and the smooth surface, the specimens are attributed to the genus *Darwinula*. The material does not allow a more detailed classification.

Suborder: Cypridocopina Jones, 1901
Superfamily: Cypridoidea Baird, 1845
Family: Cyprididae Baird, 1845
Subfamily: Cypridinae Baird, 1845
Genus *Mongolocypris* Szczechura, 1978

Mongolocypris distributa (Stankevitch in Stankevitch and Sochava, 1974) Szczechura, 1978
Fig. 6F–L

1969 *Cypridea rostrata* Galeeva; Szczechura and Blaszyk, p. 113, pl. 28, fig. 3.
1974 *Cypridea distributa* Stankevitch; Stankevitch and Sochava, p. 274, pl. 1, fig. 4.
1974 *Cypridea gigantea* Ye; Hao et al., p. 37, pl. 10, fig. 4a, b.
1978 *Mongolocypris distributa* (Stankevitch, 1974): Szczechura, p. 94, pl. 23, figs. 1–4; pl. 24, figs. 1–3; pl. 36, fig. 8; pl. 37, figs. 8, 9.

Material. More than 100 specimens, mostly complete carapaces.

Measurements. Length 1.05–1.15 mm, width 0.57 mm, height 0.57–0.675 mm.

Remarks. The large dimensions of the specimens and the specific internal structure of the valves make *M. distributa* easy to recognise. It differs from *M. tera* (Su, 1959) in having a straighter dorsal margin and the greatest height posteriorly. *M. rostrata* (Galeeva, 1955) is very similar but smaller.

Occurrence. *Mongolocypris* was described from the Nemegt Formation of Mongolia (Szczechura, 1978) and seems endemic to Asia. In Mongolia, *M. distributa* is known from the Bayn Shire to Nemegt formations (Khand, 1987). In China, it is known from the Minhe Formation in the Xining and Minhe basins (Hao, 1988), the Qingyuangang Formation, Hailar Basin (Ye, 1990) and the Shifangtai Formation, Songliao Basin (Ye, 1994).

Stratigraphical distribution. Cenomanian–Maastrichtian.

Subfamily: Talicypridinae Hou, 1982
Genus *Altanicypris* Szczechura, 1978

Altanicypris szczechurae (Stankevitch in Stankevitch and Sochava, 1974) Szczechura, 1978
Fig. 6B–C

1970 *Cypridea* sp.2; Szczechura and Blaszyk, p. 113, pl. 18, fig. 1.
1974 *Cypridea szczechurae* Stankevitch; Stankevitch and Sochava, p. 276, pl. 1, fig. 5a, b.
1974 *Cypridea obesa* Li; Hao et al., p. 42, pl. 14, fig. 3a, c.
1978 *Altanicypris szczechurae* (Stankevitch, 1974); Szczechura, p. 91, pl. 21, figs. 2–5; pl. 37, fig. 3.
1981 *Cristocypridea obesa* (Li); He et al., p. 345, pl. 2, figs. 7–9.

Material. Three complete carapaces.

Measurements. Length 0.82–0.845 mm, width 0.45–0.49 mm, height 0.45–0.475 mm.

Remarks. Several lip-bearing genera are known from the Upper Cretaceous in China and Mongolia, including *Altanicypris* Szczechura, 1978, *Talicypridea* Khand, 1977 (= *Nemegtia* Szczechura, 1978) and *Khandia* Szczechura, 1978. Our specimens are assigned to *Altanicypris* on the basis of the tumidity of the carapace and the anteroventral position of the lip; they correspond perfectly to the description given by Szczechura (1978) for *A. szczechurae*.

Hou et al. (2002) considered *A. szczechurae* as a junior synonym of *A. obesa*. However, Li (in Hao et al., 1974) described the species as *Cypridea obesa*, a name already used by Peck (1951); a rectification was never published. In the same year, *A. szczechurae* was described by Stankevitch in Stankevitch and Sochava (1974). Accordingly, *A. szczechurae* is considered to be the valid name.

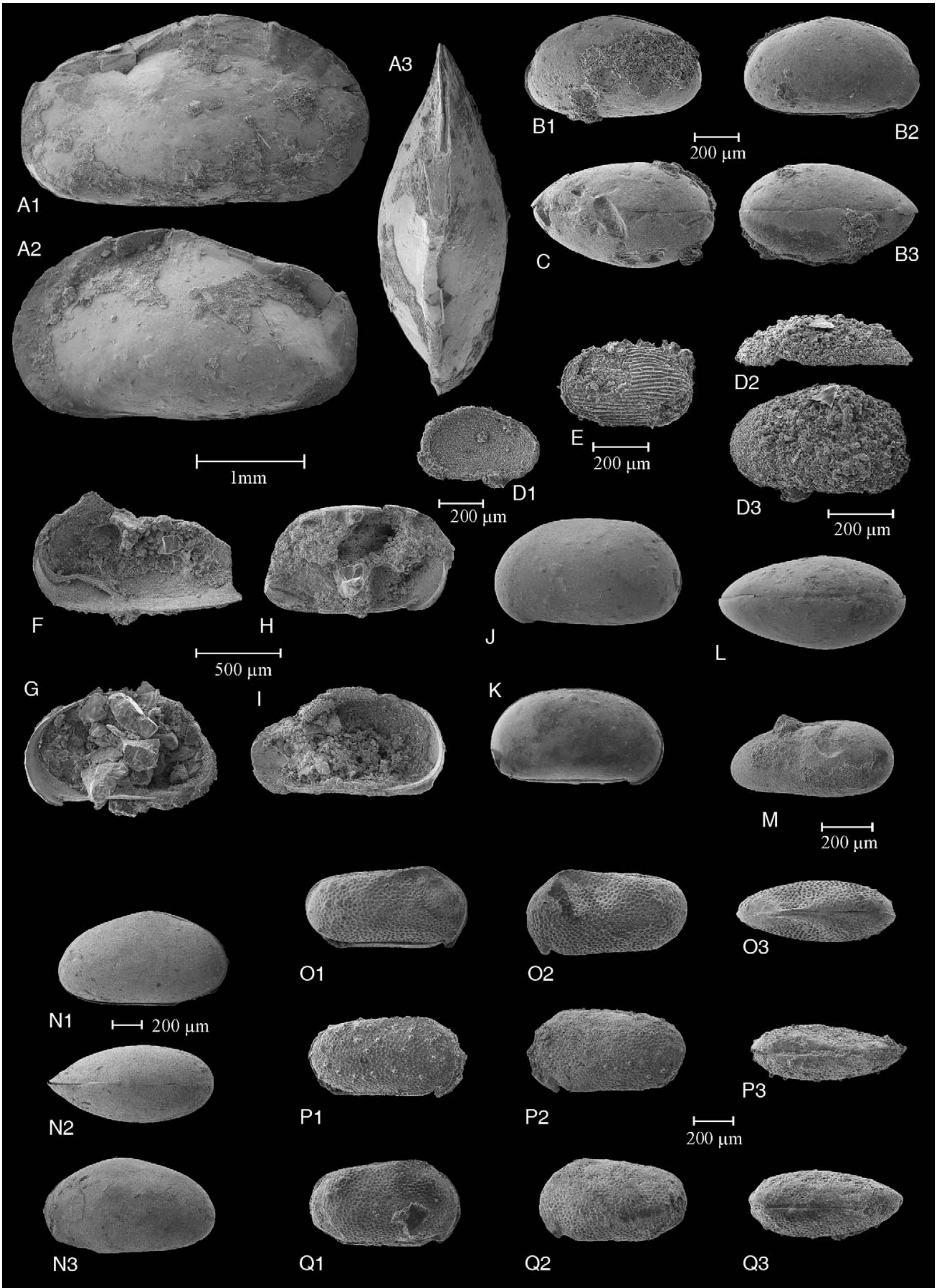
A1
A2
A3
1mm
B1
B2
B3
200 μm
C
D1
200 μm
D2
D3
200 μm
E
200 μm
F
H
500 μm
G
I
J
K
L
M
200 μm
N1
200 μm
N2
N3
O1
O2
O3
P1
P2
P3
200 μm
Q1
Q2
Q3

Occurrence. Known from the Nemegt and Barungoyot svita of Mongolia (Stankevitch and Sochava, 1974; Khand, 1987) and the Chishan Formation (Coniacian–Santonian) of Jurong, southern Jiangsu (He et al., 1981).

Stratigraphical distribution. Coniacian–Maastrichtian.

Genus *Talicypridea* Khand, 1977

1977 *Talicypridea* Khand, pp. 106–107.
1978 *Nemegtia* Szczechura, p. 96.

Talycypridea sp.
Fig. 6D

Material. One detached right valve.

Measurements. Length 0.578 mm, width 0.340 mm, height 0.347 mm.

Remarks. The specimen is poorly preserved but it still allows the determination of the genus *Talicypridea*. It differs from other lip-bearing genera by being narrower in lateral view than *Altanicypris* Szczechura, 1978, having an anteroventral lip-like extension (not medial as in *Khandia* Szczechura, 1978) and by being dorsally arched, unlike *Bogdocypris* Khand, 1994.

Occurrence. *Talicypridea* is endemic to China and Mongolia in the Upper Cretaceous, ranging from the Bayn Shire to the Nemegt formations (Khand, 2000).

Stratigraphical distribution. Cenomanian–Maastrichtian.

Subfamily: Eucypridinae Bronstein, 1947
Genus *Eucypris* Vavra, 1891

Eucypris toorojensis Khand, 1977
Fig. 6A

1977 *Eucypris toorojensis* Khand; p. 109, pl. 1, fig. 4.

Material. Five complete carapaces and two fragments.

Measurements. Length 3.25 mm, width 1.2 mm, height 1.71 mm.

Remarks. The specimens perfectly match Khand's (1977) description of *E. toorojensis*. The most characteristic features are the very large size and the well-developed marginal zone. *Eucypris*? *ampla* Zhao, 1982 is similarly large but has a distinctly different general outline.

Occurrence. The species is only known from the Nemegt Formation (Khand, 1977).

Stratigraphical distribution. Late Campanian–Early Maastrichtian.

Eucypris tostoensis Khand, 1977
Fig. 6N

1977 *Eucypris tostoensis* Khand; p. 109, pl. 1, fig. 3.

Material. Three complete carapaces and two detached valves.

Measurements. Length 1.16 mm, width 0.55 mm, height 0.666 mm (adult); length 0.844 mm, height 0.477 mm (juvenile).

Remarks. The specimens fall within the range of *E. tostoensis* Khand, 1977, the large one belonging to an adult, the smaller ones to juvenile forms. *E. gigantea* Yang in Hou et al., 1982 has a slightly more concave ventral margin. *Lycopterocypris profunda* Liubimova, 1956 is very similar but is slightly larger and has a distinctly angular bend in the anterior third of the dorsal margin.

Occurrence. In Mongolia the species is known from the Upper Nemegt svita (Khand, 1987).

Stratigraphical distribution. Early Maastrichtian.

Family: Cyprideidae Martin, 1940
Subfamily: Cyprideinae Martin, 1940
Genus *Cypridea* Bosquet, 1852

Cypridea irennorensis sp. nov.
Fig. 6O–Q

Derivation of name. After the type-locality, the Iren Nor salt lake.

Holotype. Carapace (Fig. 6O), RBINS 4378, length 0.85 mm, width 0.325 mm, height 0.45 mm.

Type locality. Outcrops at the southern border of the Iren Nor salt lake, Iren Dabasu Formation, Inner Mongolia, P.R. China.

Fig. 6. Ostracods of the Iren Dabasu Formation, Iren Nor salt lake, Inner Mongolia, P.R. China. A, *Eucypris toorojensis* (4364): 1, right, 2, left and 3, dorsal view; B, C *Altanicypris szczechurae* (4365, 4366). B, 1, left, 2, right and 3, ventral view. C, dorsal view. D, *Talicypridea* sp. (4367): 1, internal view, right valve; 2, dorsal view; 3, right view. E, *Ziziphocypris simakovi* (4368), left view. F–L, *Mongolicypris distributa* (4369–4375). F, H, internal view, left valve. G, I, internal view, right valve. J, left, K, right and L, dorsal view. M, *Darwinula* sp. (4376); N, *Eucypris tostoensis* (4377): 1, right, 2, dorsal and 3, left view. O–Q *Cypridea irennorensis* sp. nov. O, holotype (4378). P, Q, paratypes (4379, 4380): 1, right, 2, left and 3, dorsal view.

Material. Ten complete carapaces, five well preserved.

Diagnosis. Medium-sized *Cypridea*, angularly ovate in side view, laterally compressed, with a distinct beak on both valves. Greatest height close to the anterior margin, where a more-or-less pronounced depression is present. Valve surface reticulate with presence of small tubercles.

Description. Carapace medium-sized, subovate in lateral view with almost straight dorsal and ventral margins converging slightly towards the posterior; laterally compressed. Greatest height well in front of mid-length, about one-fifth length behind anterior margin, where the evenly convex anterior margin meets the almost straight posterior margin at an obtuse angle. A shallow dorsomedian sulcus is present in front of mid-length. Left valve larger than right, overlapping the latter along the entire margin. A distinct anteroventral "beak" (narrow rostrum and short alveolus) is present in both valves forming an elevated, obtuse angle with the anterior margin. Posterior margin rounded with a shallower curve in the ventral part, posterior extremity a little above mid-height. Valve surface finely reticulate with scattered small tubercles. A certain amount of variability is present within the species for the size and number of tubercles and expression of the dorsomedian sulcus.

Measurements. Length 0.775–0.85 mm, width 0.3–0.35 mm, height 0.415–0.45 mm.

Remarks. The new species strongly resembles *Cypridea* species from the Nemegt Formation, as described by Szczechura (1978); however, *C. cavernosa* Galeeva, 1955 is distinctly bigger and *C. barsboldi* Stankevitch in Stankevitch and Sochava, 1974 has more pronounced spines/tubercles, and both lack the characteristic dorsomedian sulcus of *C. irennorensis* sp. nov. *C. paucispinata* Pang in Pang et al., 1984 is more tapered anteriorly.

Occurrence. Known only from the type locality and horizon.

Superfamily: uncertain
Genus *Ziziphocypris* Chen, 1965

Ziziphocypris simakovi (Galeeva, 1955) Chen, 1965
Fig. 6E

1955 *Timiriasevia simakovi* Mandelstam; Galeeva, p. 63, pl. 15, fig. 8a, b.
1965 *Ziziphocypris simakovi* (Mandelstam); Chen, p. 28, pl. 2, figs. 6–8.

Material. Five complete carapaces.

Measurements. Length 0.509 mm, height 0.31 mm.

Remarks. *Z. simakovi* (Galeeva, 1955) strongly resembles *Z. costata* (Galeeva, 1955), which was described from the same stratigraphical level. The difference between the two species is the greater prominence of some ribs in *Z. costata*. It is unclear whether the variation in the development of the ribs justifies the division of two species. The studied specimens are closer to *Z. simakovi*.

Occurrence. *Z. simakovi* is known from the Sainshand and Bayn Shire svitas of Mongolia (Liubimova, 1956) and has been reported from the Nemegt Formation (Szczechura, 1978). In China, the species is known from the Jiadian Formation (Cenomanian–Santonian), Hubei (Ye, 1994) and from the Zouyun Formation, Shaanxi Province (Pang and Whatley, 1990).

Stratigraphical distribution. Albian–Maastrichtian.

3.2. Charophyta of the Iren Dabasu Formation

Division: Charophyta Migula, 1897
Class: Charophyceae Smith, 1938
Order: Charales Lindley, 1836
Suborder: Charineae Feist and Grambast-Fessard, 1991
Family: Porocharaceae Grambast, 1962
Genus *Porochara* Mädler, 1955

Porochara mundula (Peck, 1941) Shajkin, 1976
Fig. 8G

1941 *Aclistochara mundula* Peck; p. 291, pl. 42, figs. 7–11.
1957 *Stellatochara mundula* (Peck); Peck, p. 29, pl. 3, figs. 25–35.
1976 *Porochara mundula* (Peck); Shajkin, p. 80.
1976 *Euaclistochara mundula* (Peck); Wang et al.p. 71.
1978 *Porochara*? *mundula* (Peck) Grambast; Wang, p. 71, pl. 2, figs. 17–26.
1981 *Euaclistochara mundula* (Peck, 1941) Wang, Huang and Wang; Karczewska and Ziembinska-Tworzydlo, p. 109, pl. 38, figs. 1–6.

Material. One well preserved specimen.

Measurements. Length 0.41 mm, width 0.33 mm, ISI (= Isopolarity Index) 122; diameter of apical pore 0.113 mm, nine spiral ridges in side view.

Remarks. The characteristic shape with the truncated summit and the large apical pore make this species easy to identify and clearly place it within the genus *Porochara*.

Occurrence. *P. mundula* is abundant in mid–late Early Cretaceous sediments. In the Upper Cretaceous of China, the species has also been reported from the Honglishan and Hongshaquan formations (mid Late Cretaceous) of the Junggar Basin (Liu and Wu, 1990), the Sifangtai and Mingshui formations of the Songliao Basin, the Qingyuangang Formation of the Hailar Basin (Wang et al., 1985), several sections (Cenomanian–Campanian) in Tianzhen, Shanxi and Yuangyuan, Hebei (Liu and Pang, 1999), the Albian–Santonian of Zhejiang Province (Lin, 1989) and the Chishan Formation (Coniacian–Santonian) of the Jiangsu Province (Wang et al., 1983). Within the Gobi Basin, *P. mundula* has been described from the Nemegt Formation of Mongolia (Karczewska and Ziembinska-Tworzydlo, 1981).

Stratigraphical distribution. Barremian–Campanian.

Family: Clavatoraceae Pia, 1927
Subfamily: Atopocharoideae (Peck, 1938) emend. Grambast, 1969
Genus *Atopochara* Peck, 1938

Atopochara ulanensis Kyansep-Romashkina, 1975
Figs. 7, 8A–F.

1975 *Atopochara ulanensis* Kyansep-Romashkina; p. 190, pl. 2, fig. 2a, b; pl. 3, figs. 1, 2.
1981 *Atopochara ulanensis* Kyansep-Romashkina; Karczewska and Ziembinska-Tworzydlo, p. 108, pl. 25, fig. 1; pl. 31, figs 1–3.

Material. More than 100 utricles, only a few well preserved.

Description. The gyrogonites, represented by internal moulds, show a summit stretched into a neck and are covered by a utricle. The subglobular utricle shows a three-rayed symmetry and consists of three groups of 11 cells (Fig. 7). The cell a2 has not been observed in any of the specimens. In summit view, 12 spirally wound cells are visible, covering more than half of the utricle.

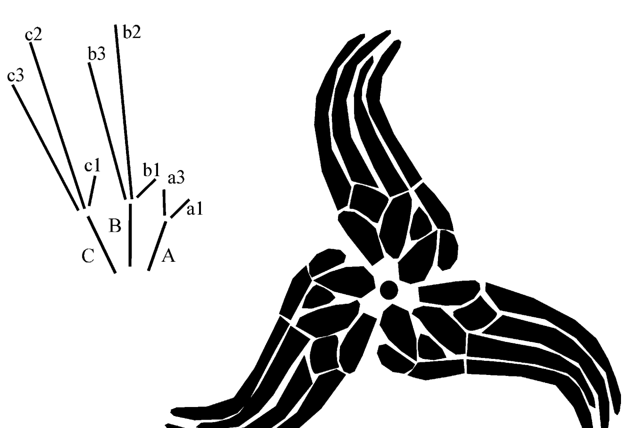

Fig. 7. Interpretation of the utricular structure of *Atopochara ulanensis* Kyansep-Romashkina, 1975.

Measurements. Length 0.84–0.98 mm, width 0.84–0.965 mm.

Remarks. The original description of *A. ulanensis* did not include a schematic drawing of the utricle structure and the illustrations of the type specimens were limited to line drawings, flaws which have led to a discussion on the validity and classification of the species that is currently unresolved.

Karczewska and Ziembinska-Tworzydlo (1983) put *A. ulanenis* in synonymy with *A. restricta* Grambast-Fessard, 1980. They used this as a basis for revising the age of the Nemegt Formation to Early Campanian. Martin-Closas (1996) followed the view of the Polish charophytologists and put the two species in synonymy, although he gave priority to *A. trivolvis* var. *restricta*. According to Martin-Closas and Schudack (1997), *A. trivolvis* var. *restricta* was isolated in the intercontinental basins of Asia before the anagenetic transformation of *A. restricta* to *A. multivolvis* in Europe and North America, where it persisted during the Late Cretaceous. However, this geographical separation needs to be reviewed because *A. multivolvis* has been reported from Asia (Kyansep-Romashkina, 1980; Gereltsetseg, 1998, 2001). The view of Martin-Closas and Schudack (1997) on the taxonomy of *A. ulanensis* in particular, and the *Perimneste*-*Atopochara* lineage in general, is not accepted by Feist and Wang (1995). These authors considered *A. ulanensis* as a clearly distinct species that represents a side branch of the *Perimneste*–*Atopochara* evolutionary lineage. Such a view was previously proposed by Kyansep-Romashkina (1982), who described *A. barungoiotica* as an intermediate form between *restricta* and *ulanensis*. However, based on the original description and illustrations, it is impossible to differentiate *A. barungoiotica* Kyansep-Romashkina, 1982 from *A. ulanensis*. Even Kyansep-Romashkina failed to mention the characteristics that separate the two species. A revision of the type-material, with a comparison of the material attributed to *A. ulanensis*, *A. barungoiotica* and *A. restricta*, is needed to solve the current taxonomic problems. However, such a systematic study is beyond the scope of the present paper.

The studied specimens match perfectly the original description and the illustrations, as given by Karczewska and Ziembinska-Tworzydlo (1981), of *A. ulanensis*. A detailed comparison of the structure of the utricle of *A. ulanensis* (Fig. 7) with *A. restricta* (Grambast-Fessard, 1980, fig. 1b) shows that both species have the same number of cells and the same general structure. The main difference between both is the length of the cells. In *A. ulanensis*, the basal cells are shorter than in *A. restricta*, not reaching the equator of the utricle.

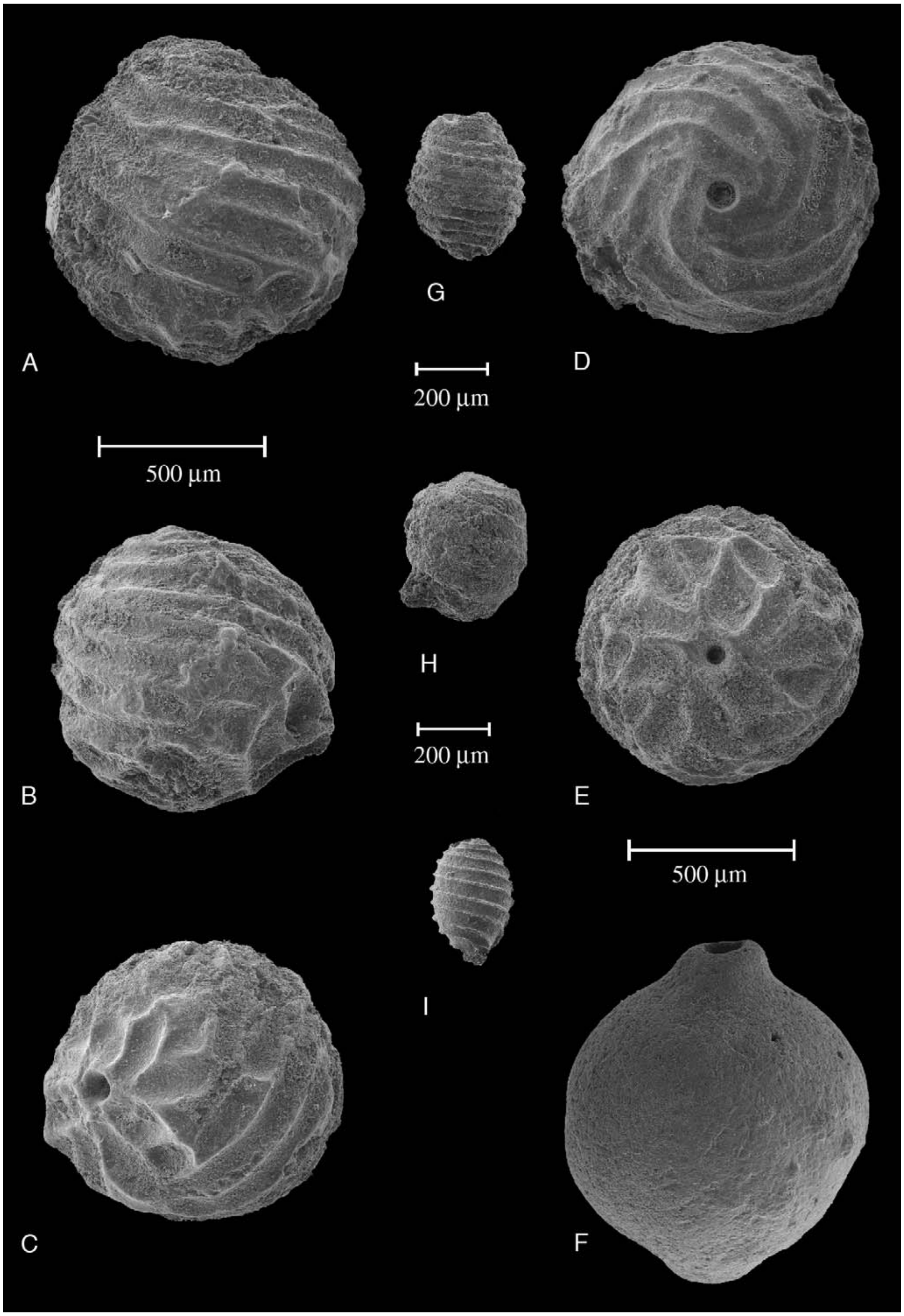

Fig. 8. Charophytes of the Iren Dabasu Formation, Iren Nor salt lake, Inner Mongolia, P.R. China. A–F, *Atopochara ulanensis* (4381–4386). A, lateral (4381), B, lateral (4384), C, oblique lateral (4385), D, apical (4383), E, basal (4382) view. F, gyrogonite (4386); G, *Porochara mundula*, lateral view (4387). H, *Nemegtichara prima*, lateral view (4388). I, *Mesochara stankevitchii*, lateral view (4389).

Inevitably, the upper spiralling cells are more elongated. Another difference is the presence of a suppressed cell a2 on some specimens of *A. restricta* (Grambast-Fessard, 1980, pl. 1, fig. 5). Therefore the specimens are attributed to *A. ulanensis*.

Occurrence. *A. ulanensis* is endemic to Asia and was first described from the Ulan Bulak locality, Nemegt Formation (Kyansep-Romashkina, 1975). Subsequently, it has been observed in several other localities of the Nemegt Formation within the Gobi Basin (Karczewska and Ziembinska-Tworzydlo, 1981). In China, the species is known from strata of Campanian–Maastrichtian age, for example, the Sifangtai and Mingshui formations of the Songliao Basin and the Qingyuangang Formation of the Hailar Basin (Wang et al., 1985).

Stratigraphical distribution. Campanian–Maastrichtian.

Family: Characeae Richard ex Agardh, 1824
Genus *Nemegtichara* Karczewska and Ziembinska-Tworzydlo, 1973

Nemegtichara prima Karczewska and Ziembinska-Tworzydlo, 1973
Fig. 8H

1973 *Nemegtichara prima* Karczewska and Ziembinska-Tworzydlo; pp. 54–55, pl. 7, fig. 3.

Material. One well preserved specimen.

Measurements. Length 0.42 mm, width 0.35 mm, ISI 118, six spiral ridges in side view.

Remarks. The typical apical structure of *Nemegtichara* makes it easy to identify. Based on the size and general outline, the specimen was attributed to *N. prima*.

Occurrence. The species was first described from the White Beds (Palaeogene) of the Nemegt Basin (Karczewska and Ziembinska-Tworzydlo, 1973). Its range was extended by numerous specimens found within Late Cretaceous deposits in China: for example, the Nanxiong Formation (Late Cretaceous) in the Nanxiong Basin, Guangdong Province (Huang, 1988), the Shanshui Formation (Late Cretaceous, Santonian) in the Shanshui Basin, Guangdong Province (Huang and Zhang, 1984), the Sifangtai and Mingshui formations (Late Cretaceous) in the Songliao Basin, the Qingyuangang Formation (Late Cretaceous) in the Hailar Basin (Wang et al., 1985), the Chishan Formation (Coniacian–Santonian) in Jiangsu Province (Wang et al., 1983), the Taizhou (Campanian) and Funing (Paleocene) formations in Jiangsu Province (Huang and Zhao, 1989) and the Wujiashan section (Cenomanian–Campanian) in Tianzhen, Shanxi, Yuangyuan, and Hebei (Liu and Pang, 1999).

Stratigraphical distribution. Coniacian–Paleocene.

Genus *Mesochara* Grambast, 1962

Mesochara stankevitchii Kyansep-Romashkina, 1975
Fig. 8I

1975 *Mesochara stankevitchi* Kyansep-Romashkina; pp. 195–196, pl. 4, figs. 1a, b, 2a, b.

1981 *Mesochara stankevitchii* Kyansep-Romashkina; Karczewska and Ziembinska-Tworzydlo, pp. 117–118, pl. 29, figs. 1–3, 6, 7.

Material. One well preserved specimen.

Measurements. Length 0.37 mm, width 0.24 mm, ISI 152, nine spiral ridges in side view.

Remarks. Kyansep-Romashkina (1975) erected *M. stankevitchii* to include specimens similar to *Mesochara voluta* Peck, 1937, differing from those described by Peck in having a strongly elongated basal part. Peck (1957) had already mentioned that the specimens attributed to *M. voluta* could represent more than one species. The separation of *M. stankevitchii* from *M. voluta* was confirmed by Karczewska and Ziembinska-Tworzydlo (1981).

Occurrence. The species was first described from the Barungoyot Formation at the Altan Ula locality (Kyansep-Romashkina, 1975). Later it was reported from the Nemegt Formation at several localities (Karczewska and Ziembinska-Tworzydlo, 1981). In China, it is known from the Chishan Formation, Jiangsu (Coniacian–Santonian) (Wang et al., 1983) and from the first member of the Taizhou Formation, Jiangsu (Campanian) (Huang and Zhao, 1989).

Stratigraphical distribution. Coniacian–Maastrichtian.

4. Discussion and stratigraphical implications of the micropalaeontological data

Both the ostracod and charophyte assemblages of the Iren Dabasu Formation have been described in the literature, but precise details on the localities or sections yielding the microfossils were not given. The data presented here is therefore the first documentation of charophyte and ostracod taxa from the type locality of the Iren Dabasu Formation, the Iren Nor dinosaur site. Pang and Whatley (1990) listed the following ostracods from the Iren Dabasu Formation (cited as the Erliandabusu Formation): *Cypridea tera* Su (now placed in *Mongolocypris*), *Talicypridea obesa* Li, *Lycopterocypris cuneata* (Tsao), *Lycopterocypris profunda* Liubimova, *Theriosynoecum*? *erlianensis* Zhang. The ostracod assemblage of the Iren Dabasu Formation at the Iren Nor dinosaur site is very similar but more diverse. The charophyte assemblage described by Liu (1987, pp. 131–133), despite the species richness, only has *Nemegtichara prima* in common with that described herein.

The micropalaeontological assemblage of the Iren Dabasu Formation at the Iren Nor site shows great affinity with assemblages from the Chishan

(Coniacian–Santonian) Formation and the first member of the Taizhou Formation (Campanian) in the North Jiangsu Basin (He et al., 1981; Wang et al., 1983; Huang and Zhao, 1989), the Sifangtai and Mingshui formations (Campanian–Maastrichtian) of the Songliao Basin (Wang et al., 1985; Ye, 1994) and the Qingyuangang Formation (Campanian–Maastrichtian) of the Hailar Basin (Wang et al., 1985; Ye, 1990). The ages of these Chinese formations have been independently established, based on palynology (Li and Liu, 1994; Zhang and Li, 2000). The greatest resemblance, however, is with the ostracod (Szczechura, 1978; Khand, 1987) and charophyte (Kyansep-Romashkina, 1975; Karczewska and Ziembinska-Tworzydlo, 1981) assemblages of the Nemegt Formation. Based on the presence of the hadrosaurine dinosaur *Saurolophus* (cf. supra), the age of the Nemegt Formation is estimated as Early Maastrichtian (Jerzykiewicz and Russell, 1991). Although this age is based on vertebrate evidence, it is considered reliable (Hicks et al., 1999, p. 831). Based on charophyte evidence, in particular the presence of *Atopochara ulanensis*, Karczewska and Ziembinska-Tworzydlo (1983) estimated the Nemegt Formation to be no younger than Early Campanian. Commonly, clavatoraceans are very useful for biostratigraphical purposes because they allow accurate age estimations of continental deposits. However, *A. ulanensis* is an endemic Asian species, occurrences of which have not yet been calibrated with the international time scale, and (as mentioned above) its systematic position is unclear. Karczewska and Ziembinska-Tworzydlo (1983) proposed a Santonian age for the Barun Goyot Formation; however, radiometric calibrations (Shuvalov, 2000) have provided a Campanian age for this formation. Since the Nemegt Formation overlies the Barun Goyot (Gradzinski et al., 1977, fig. 12), it must be younger; accordingly, we regard the age estimation for the Nemegt Formation as proposed by Karczewska and Ziembinska-Tworzydlo (1983) as incorrect.

The dominance of the genus *Mongolocypris*, together with the occurrence of lip-bearing ostracods such as *Talicypridea* and *Altanicypris* (Gou and Cao, 1983; Hao et al., 1983; Khand, 2000), places the assemblage studied within the Late Cretaceous. The stratigraphical ranges of the charophyte and ostracod taxa limit the age to the Campanian–Maastrichtian interval. This is supported by the above-mentioned correlations with the Chinese Upper Cretaceous formations. Based on the good correlation with the Nemegt Formation of the Gobi Basin in Mongolia, the age of the Iren Dabasu Formation can probably be refined to the latest Campanian–Early Maastrichtian.

In conclusion, the age of the Iren Dabasu Formation can be estimated as Campanian–Maastrichtian, confirming the opinion of Chinese scientists (Table 2) and calling into question the earlier age estimations based on vertebrate evidence (Jerzykiewicz and Russell, 1991; Currie and Eberth, 1993; Godefroit et al., 1998). The good correspondence of the micropalaeontological data with that of the Nemegt Formation (Table 3) raises questions about the previous correlations with the Bayn Shire Formation, based on vertebrate evidence (Currie and Eberth, 1993). Although a few of the observed micropalaeontological taxa do occur in the Bayn Shire Formation, the entire assemblage is definitely more characteristic of the Nemegt Formation and equivalent Chinese strata.

5. Sedimentology

The sedimentology of the Iren Dabasu Formation is discussed here on the basis of new observations from exposures around the Iren Nor salt lake (Fig. 3 for the exact locations of the exposures). In general, exposure on the vast plain with steppe vegetation is poor to mediocre. Good exposures are limited to isolated spots in the landscape where the relief is slightly steeper, or to small gullies where the Quaternary cover is more deeply eroded. Consequently, outcrop faces are weathered and often covered by a pebbly lag in which fossils are concentrated. The small gullies provide exposures with fresh faces, but are short-lived as they are quickly filled with recent deposits. The only long-lived exposure of good quality has been found within a large river valley on the northern side of the lake (ERHVAL on Fig. 3). In the outer bends of the river channel, which is dry during summer, the sediments are exposed along fresh vertical faces several metres high and several tens of metres long.

Based on the exposure conditions, the nature of the strata and the fossil content, the outcrop area around the Iren Nor salt lake can be divided into a northern and a southern part. The northern part includes all the exposures in the dry river valley north of the lake. The southern part comprises the exposures on the southwestern edge of the lake and in an area about 4 km east of the lake. The location of the exposures on the southwestern edge of the lake is within the area containing collection sites 131, 135, 136 and 138 of the Central Asiatic Expeditions of the American Museum of Natural History (AMNH); the locality east of the lake is close to collection sites 140–145 and 149 of the AMNH (Gilmore, 1933, p. 26).

In spite of the numerous expeditions to the Iren Nor region, the work of Currie and Eberth (1993) was the first sedimentological study on the Iren Dabasu Formation. It was based on outcrops on the southwestern border of the lake (Currie and Eberth, 1993, p. 131, fig. 3) corresponding to outcrop ERH00/II herein. Currie and Eberth (1993) divided the formation into coarse- and fine-grained members, representing channel and inter-channel deposits, respectively. The series of tabular hills in the present-day landscape reflects this lithological division: the erosion-resistant, coarse-grained deposits form small plateaus, while the easily-eroded, fine-grained deposits form the slopes between them. For convenience, the same division will be maintained in the description of the different facies recognised within the Iren Nor field area.

5.1. Facies description

5.1.1. Coarse-grained deposits

C1. This facies represents the coarsest facies found in the field area as it consists of massive to horizontally-stratified conglomerates and cross-bedded very coarse sands (Fig. 9). These lithologies are only exposed in the northern part. They have an unknown lateral extent and their thickness exceeds 20 m. The conglomerates and coarse sands of this facies typically show a fining-upward trend. Palaeocurrent measurements reveal a unidirectional current towards the north. Downstream accretion macroforms (as defined by Miall, 1996) have been recognised within the coarse sands of this facies. Zones of intense synsedimentary deformation were observed (Fig. 10), ranging from wavy laminations to zones of complex disharmonic folds. These structures can be classified as convolute laminations and occur within the coarse, sandy deposits. Similar deformation has been observed in recent flood deposits of braided river systems (McKee et al., 1967), where they develop within the main channel belt in a late stage of the flood when the current velocities slow down and the sediment acts as a quicksand. Within the C1 facies, numerous silicified wood fragments, attributable to gymnosperms, occur. The poor preservation of these fragments prohibits a more detailed classification.

C2. Most of the coarse layers in the southern part that form the plateaus of the tabular hills belong to this facies. Currie and Eberth (1993) recognised this facies and characterised it as erosionally based, sandy deposits composed of fining- and thinning-upward sets of large-scale trough cross-bedding, horizontal-planar and ripple-laminations, with locally abundant vertebrate fossils at the base. This facies was deposited in broad, shallow channels (4 m high and up to 1 km wide) that can be observed within the exposures. Numerous measurements of the trough-shaped cross-beds were made at different stratigraphical levels within this facies. In spite of the strongly varying measurements, a dominant palaeocurrent direction to the southwest was detected (Fig. 11).

C3. In exposure ERH00/II, one channel deposit proved rich in *Pseudohydria gobiensis* MacNeill, 1936. The mode of preservation of these bivalves is variable and includes internal and external moulds and natural casts. On one specimen, the original nacreous layer is preserved. Most of the specimens however consist of a single shell. The same layer proved rich in charophytes and ostracods, as described above. In contrast to Facies C2, this deposit is dominantly composed of calcareous clasts, which are reworked palaeosol nodules.

5.1.2. Fine-grained deposits

F1. According to Currie and Eberth (1993), the fine-grained members comprise two facies types. The first consists of tabular bodies of thinly bedded heterolithic sand-, silt-, and claystone. These deposits pass laterally into the coarse-grained members and are exposed in the southern part of the field area.

F2. The second type of fine-grained member recognised by Currie and Eberth (1993) comprises massive

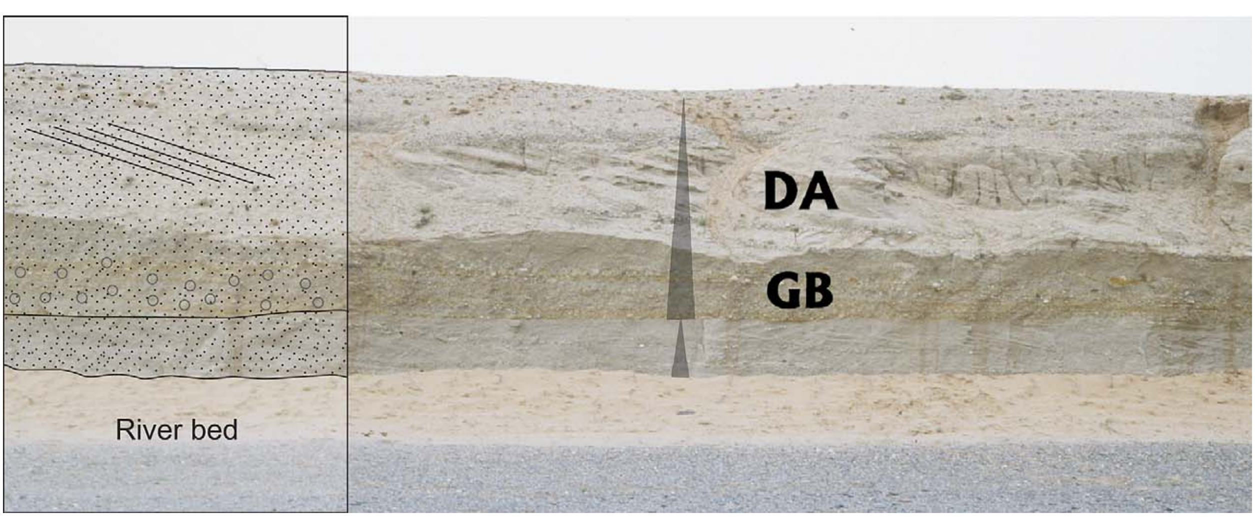

Fig. 9. Overview of part of outcrop ERHVAL 6 (height 5 m, length 50 m), showing two in-channel fining-upward cycles within Facies C1; a cycle starts with a gravelly bedform (GB), composed of horizontally-stratified gravel beds, that grades into a sandy, downstream accretion macroform (DA) composed of dominantly planar sandy cross-beds (symbols and terms after Miall, 1996).

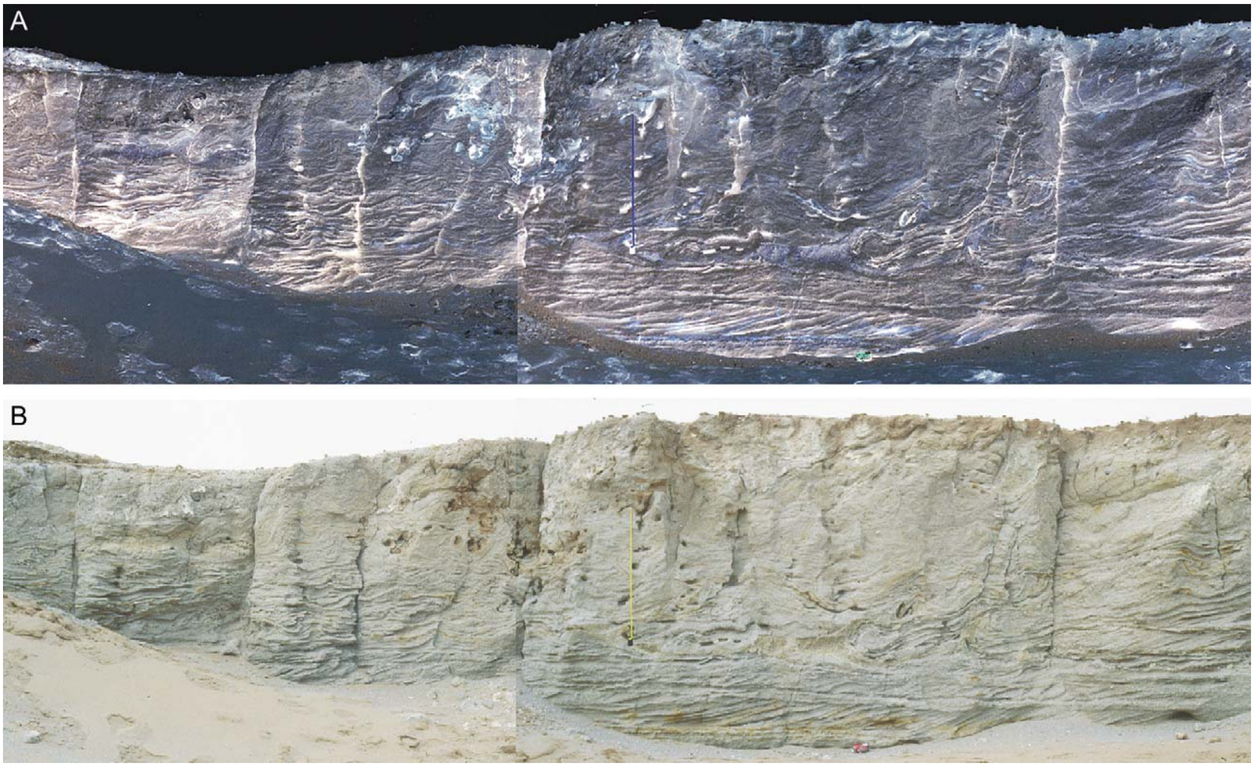

Fig. 10. Convolute laminations in negative (A) and positive (B) view as frequently seen in outcrops along the dry river valley on the northern part of the lake (part of outcrop ERHVAL 9: length 10 m, height 2.5 m).

silt- and claystones with caliche nodules, vertebrate eggshells, in situ eggs in nests and other features of palaeosol development (gleying, root traces and clay-lined peds).

F3. A third type of fine-grained deposit consists of finely-laminated silts and clays (Fig. 12B) containing ostracods and charophytes. The colour of these deposits varies between grey (5Y 8/1) through moderate yellowish brown (10YR 5/4) to dark reddish brown (10R 3/4). Within the red layers of these fines, calcareous nodules a few centimetres in length occur. The colour of the nodules varies from dark yellowish orange (10YR 6/6) on the outside to dark yellowish brown (10YR 4/2) inside. These thinly bedded sediments occur as the infill of a channel-like incision in exposure ERH00/III (Fig. 12A). At the edge of the channel, a small slump deposit was seen (Fig. 12C). Simple synclinal folds with vertical axes occur frequently in this facies (Fig. 12D); these structures can also be classified as convolute laminations, a term that is purely descriptive and has no genetic implications. Indeed, these convolute laminations differ from the structures observed within Facies C1. The latter are syndepositional features while the structures in the finely-laminated F3 facies are postdepositional, as they deform the red palaeosol horizons with calcareous nodules that are normally subhorizontal. Such features result from an upward flow generated by different mechanisms (Chakrabarti, 1977). The possibility that these deformations formed under the weight of passing dinosaurs (= dinoturbation) cannot be excluded.

F4. The fine-grained deposits observed in the northern part make up Facies F4. These massive mudstones are limited to thin (<20 cm) infills of scour structures or drapes on top of coarser deposits (Fig. 13).

5.1.3. Palaeosols

Throughout the succession, several hiatuses, characterised by palaeosol development, occur. In outcrop ERH00/I, a nest of dinosaur eggs was found within a palaeosol horizon. Only calcretic palaeosols were recognised throughout the field area. The thickness of the profile varies from 10 cm in the most condensed section to nearly 1 m in the thickest sections. In the condensed sections, the calcrete nodules occur within a red horizon. The pattern of the thickest section, as observed in outcrop ERH00/I (Fig. 14), is slightly different. Considering the presence of a channel deposit with an erosive base on top of the profile, the section is incomplete; it starts with a horizon of calcareous nodules (Bk), the size and the lithification of which vary depending on the degree of soil development. The next horizon is characterised by its reddish colour (10R 3/4). The profile terminates with a brown horizon (10YR 5/4), bordered at the top by a very thin, black manganese-rich zone. These horizons, characterised by an alluvial accumulation of sesquioxides, form the Bs

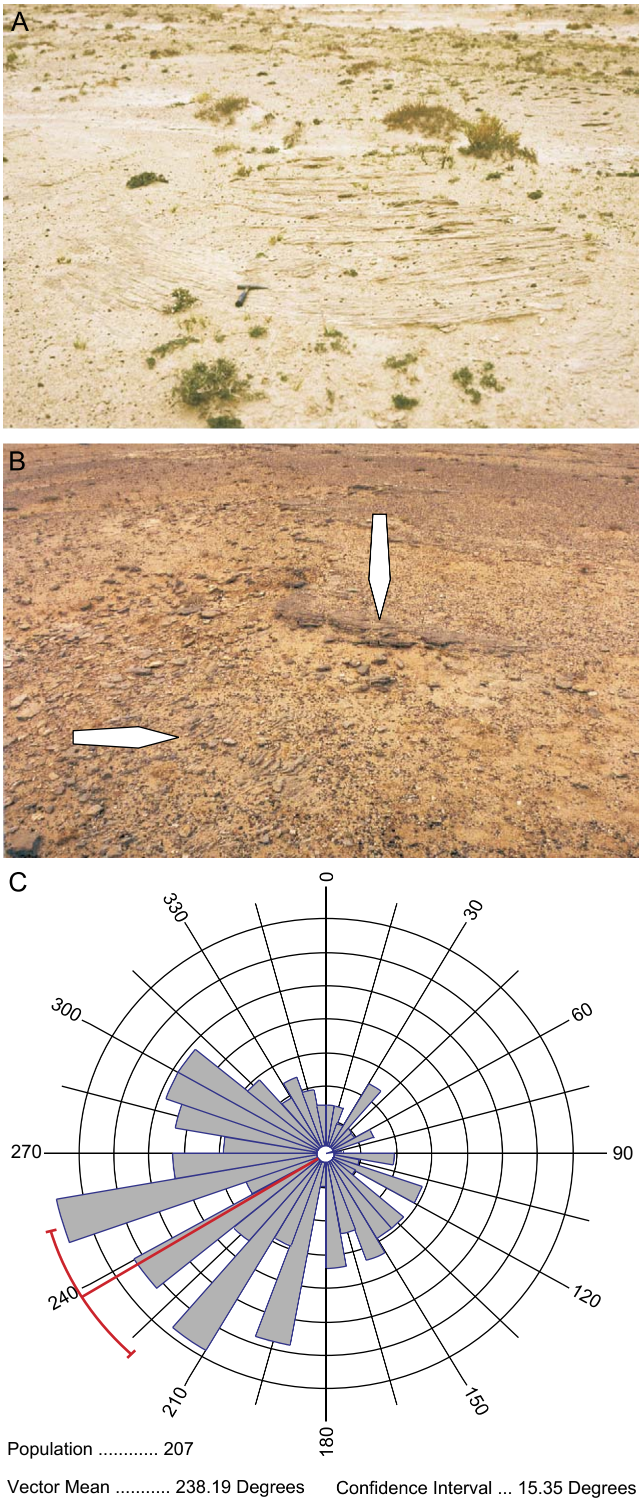

Fig. 11. Overview of the trough-shaped cross-beds observed in the southern part. A, exceptionally well-exposed trough-shaped cross-bed in a horizontal section in outcrop ERH00/II. B, normal exposure of trough-shaped cross-beds in a horizontal section in outcrop ERH01/V, with arrows indicating two different directions that crop out side by side. C, rose diagram with all the measurements made of trough-shaped cross-beds throughout the southern area.

horizon. On average, 80% of the clay minerals within the profile are smectites. Throughout the entire profile, slickensides occur as a consequence of shrinking and swelling of the soil. Such features have not been observed within the condensed sections.

The calcisols, according to Mack et al. (1993), occur throughout the entire field area and indicate a semi-arid climate with an annual precipitation limited to 760 mm (Royer, 1999). The more condensed profiles, ferric calcisols, represent uniformly dry settings, whereas the thick soil profile, gleyed vertic calcisol, clearly represents a setting on the floodplain that underwent regular changes in humidity, causing shrinking and swelling of the clay and gley features such as a manganese enrichment. These differences in humidity reflect different palaeohydrological conditions that are most likely related to the ancient topography.

5.2. Taphonomy

All the vertebrate sites are restricted to the southern part. So far, no complete, articulated skeletons have been found at Erenhot. The dinosaur fossils are found in bone beds composed of disarticulated to partially associated dinosaur bones. The Sino-Belgian team excavated three major sites (labelled by the year of excavation on Fig. 3).

Productive horizons of vertebrate fossils in fluvial settings occur in two predictable contexts (Behrensmeyer, 1982). The first and best known context for fossil vertebrate material is in association with coarse-grained channel deposits. Productive horizons are often also associated with sedimentary contacts representing temporary land surfaces (occasionally with well-developed palaeosols) in fine-grained floodplain sediments.

Both contexts have yielded rich dinosaur assemblages in the Iren Dabasu Formation. The bone bed excavated in 1995 yielded a monotaxic assemblage associated with channel sediments and is a typical example of the channel-lag mode of attritional vertebrate assemblages in fluvial channels (Behrensmeyer, 1988). The bone beds excavated in 2000 and 2001 are multitaxic assemblages associated with overbank mudstones; they represent attritional vertebrate assemblages on the floodplain. The taxonomic composition is variable for each locality and probably reflects in-life heterogenous faunal distributions on the floodplain (Gilmore, 1933; Currie and Eberth, 1993). Within the bone beds of 2000 and 2001, features of palaeosol development were recognised. Bone bed 2000 falls within the thickest profile of palaeosol development recognised in the field area (see previous section). The bones recovered from this bed vary in colour depending on the soil horizon in which they were found. Some of the bones were even encrusted with calcic or ferric material. According to Behrensmeyer (1982),

Fig. 12. A, overview of abandoned channel infilled with finely-laminated sediments; dotted line indicates base of channel. B, detail of Facies F3; arrow indicates calcareous nodule within a red layer. C, slump observed near base of abandoned channel. D, synsedimentary deformation in Facies 3; arrow indicates deformed palaeosol horizon with calcrete nodules.

the preservation of vertebrate bones on floodplains was greatly enhanced if the substrate was soft enough to permit downward movement of the bones by trampling and if it promoted vegetation growth that buried the bones. Both conditions are fulfilled at bone bed 2000. As discussed before, the palaeosol at this site demonstrates intervals of increased humidity that would have softened the sediments and promoted the growth of vegetation, both factors increasing the chances of preservation of dinosaur bones.

Due to their mode of preservation, the bone beds associated with floodplain sediments, with bones throughout the entire soil profile, are generally thicker than those associated with channel deposits, where the bones occur as a basal lag deposit. In the latter, all the bones are horizontally orientated, whereas in the former, vertically orientated bones can be seen, most likely as a result of their mode of burial (trampling, bioturbation).

5.3. Discussion

Three different types of channel deposits are recognised (Table 4). The coarse-grained Facies C1, cropping out in the northern part, forms the first type. The gravels form a basal gravelly bedform (GB) that is overlain by a series of in-channel sandy bars arranged in a downstream accretion macroform (DA). Judging by the coarse granulometry and the great thickness, these deposits most likely represent the principal channel of the system. The coarse-grained deposits of the southern part, forming plateaus in the present-day landscape, fall within the description of Currie and Eberth (1993) and represent the minor channels of the system. The channel deposit rich in intraclasts, bivalves, charophytes and ostracods represents Type 3. This deposit attests to a situation whereby the supply of intraformational clasts, due to erosion of floodplain sediments, exceeds the supply of extraformational detritus, such as occurs

Fig. 13. Detailed view of outcrop ERHVAL 8 (length 15 m, height 1.5 m), a scour hollow (HO), formed at the confluence of two channels, has eroded the top of the underlying sandy bar (Sp). During the next low-water stand, an in-channel pond formed in this hollow with sedimentation of suspended material. With the next rise in water level, a new cycle started, with the sedimentation of a gravelly bedform (Gh) on top of these deposits. Symbols and terms after Miall (1996).

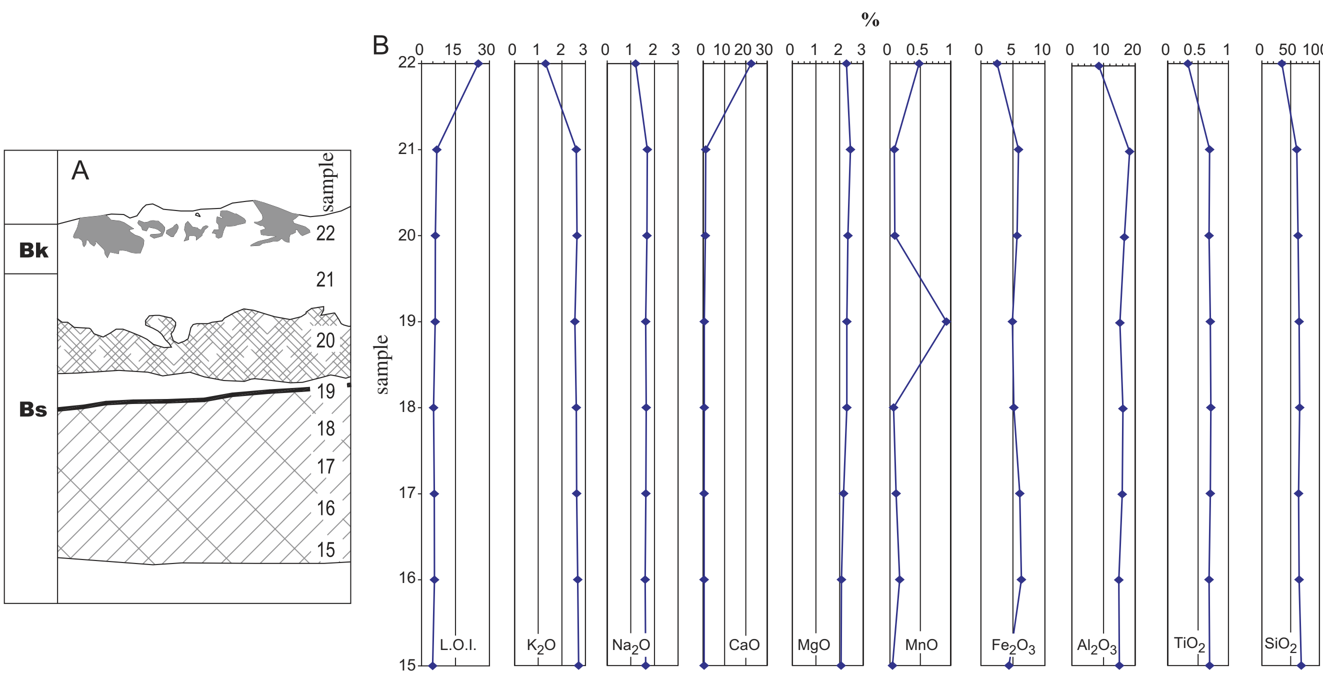

C

Sample	L.O.I.	K_2O	Na_2O	CaO	MgO	MnO	Fe_2O_3	Al_2O_3	TiO_2	SiO_2	Total
22	25.09	1.31	1.20	22.51	2.29	0.48	2.54	8.55	0.33	34.56	98.86
21	6.76	2.61	1.70	1.15	2.46	0.07	5.88	18.22	0.69	60.64	100.18
20	6.11	2.64	1.68	1.05	2.35	0.08	5.64	16.60	0.68	62.92	99.75
19	6.03	2.55	1.63	0.51	2.31	0.93	4.91	15.16	0.70	64.76	99.49
18	5.30	2.61	1.65	0.48	2.31	0.06	5.14	16.14	0.71	65.73	100.13
17	5.62	2.63	1.64	0.44	2.17	0.10	6.06	15.89	0.70	63.84	99.09
16	5.73	2.67	1.61	0.42	2.08	0.16	6.32	14.83	0.68	64.83	99.33
15	4.93	2.71	1.63	0.41	2.06	0.04	4.39	15.00	0.69	68.38	100.24

Fig. 14. Schematic drawing of a palaeosol profile (thickness 1 m) as observed in outcrop ERH00/I. A, numbers indicate positions of samples. Graphs (B) and table (C) show results of the chemical analyses of the samples. Bk, soil horizon with carbonate nodules; Bs, soil horizon enriched in sesquioxides, L.O.I., loss on ignition.

Table 4
Description and interpretation of the facies observed within the Iren Dabasu Formation (* indicates facies described by Currie and Eberth, 1993)

Facies	Description	Interpretation
Coarse		Channel deposit
C1	Massive to horizontally-stratified gravels and planar cross-bedded, very coarse sands, >20 m thick, lateral extent unknown; organised in fining- upwards, DA macroforms, silicified wood logs	Major channel infill
C2*	Coarse-grained deposits, erosionally based, 4 m high, up to 1 km wide, fining- and thinning- upward sets of large-scale, trough cross-bedding, horizontal-planar and ripple lamination; locally, base enriched in dinosaur bones	Minor channel infill
C3	Intraclast-rich, coarse-grained deposit, rich in fossils - bivalves, ostracods and charophytes	Minor channel infill after avulsion
Fine		Inter-channel deposit
F1*	Tabular bodies of thinly bedded heterolithic sand-, silt- and claystone; planar beds of ripple lamination, horizontal stratification; pass laterally into coarse-grained deposits	Sheet splays emanating from the broad and shallow primary channels
F2*	Massive sandy siltstone and claystone deposits with palaeosol development (calcrete nodules, red coloring, root traces), eggs in nests	Suspension deposits in a variety of floodplain settings
F3	Thinly bedded silts and clay with charophytes and ostracods	Abandonned channel infill
F4	Massive silts and clays, of a limited lateral and vertical extent, interbedded within channel deposits	In-channel deposits at low-water stages

during an avulsion event when the river searches a new path on the floodplain, reworking its own sediment. This facies strongly resembles the intraformational conglomerates of the Bayn Shire Formation (Jerzykiewicz and Russell, 1991).

Palaeocurrent measurements in the northern part indicate a northward palaeoflow. Considering the quality of the outcrops and the uniformity of the measurements, the northward flow direction for the main channel belt seems highly reliable. Based on the trough cross-beds within the coarse members in the southern part, Currie and Eberth (1993) derived a unidirectional flow to the northwest, with ancillary flow to the northeast and southwest for the minor channels. This corresponds well with the flow direction in the main channel. The new measurements made in this study, indicating a palaeocurrent to the southwest (Fig. 11), seem to be biased towards the ancillary southwesterly flow direction. The mediocre outcrop conditions in the southern part often make it hard to establish the trough axis correctly and can account for the different results. Currie and Eberth (1993) also mentioned a strongly localised variation in palaeocurrent in their study.

According to Currie and Eberth, the fine-grained members comprise two types of deposits, Facies F1 and F2. They interpreted the first type as sheet splays emanating from the primary river channels and the second type as suspension deposits on the floodplain with depositional hiatuses represented by calcrete palaeosols. However, the fossil content of these massive floodplain deposits is not limited to dinosaur eggs; two extensive bone beds found within these massive floodplain deposits proved very rich in disarticulated dinosaur remains.

In addition to those recognised by Currie and Eberth (1993), two more types of fine-grained deposits were found. A third type of fine-grained deposit is represented by the very thinly bedded clays and silts (Fig. 12) infilling an abandoned channel that formed a temporary pond on the floodplain. The calcrete palaeosols developed within these pond deposits attest to periods of subaerial exposure of the sediments. The ostracod fauna is dominated by cypridoidean species, which have desiccation-resistant eggs (Horne and Martens, 1998) and were able to live in temporary water-bodies. In modern environments, "giant" ostracods (i.e., several mm long) only occur in fish-free water-bodies, and the occurrence of the large ostracod *Eucypris toorojensis* probably indicates such a habitat, most likely of a temporary character. Currie and Eberth (1993) mentioned the occurrence of a tabular dolomite bed, which they interpreted as a playa deposit. During the fieldwork of the SBDE, no such deposit was observed but it is noteworthy that such lithologies are also indicative of temporary water-bodies.

The silts and clays interbedded within the coarse-grained channel deposits exposed in the northern part form the fourth type of fine-grained deposit. They represent small ponds of stagnant water in the riverbed during stages of low water-level. In recent settings, such scours occur at the confluence of two channel braids where the erosive power of the river increases. Unlike the other fine-grained deposits, they must be seen as in-channel and not as floodplain deposits.

5.4. Interpretation

The Iren Dabasu Formation represents a Late Cretaceous braided river system. The principal channel in the northern part of the ancient system can be characterised as a unidirectional, multichannel flow with large gravel and coarse-grained sand bars. No lateral accretion surfaces were observed, only downstream accretion. Minor channels in the southern part represent braided channels (Currie and Eberth, 1993) on the basis of their shallow and broad nature. The outcrops in the northern part are limited to a modern dry river valley, so that the lateral extent of the major channels could not be defined; the thickness of the channel deposits exceeds 20 m. The limited occurrence of fine-grained deposits in the northern part corresponds well with the classical models of braided river deposits (e.g., Williams and Rust, 1969; Rust, 1975; Miall, 1977; Reinfelds and Nanson, 1993). However, the large volume of fines within the southern part seems to contradict the classical models, a problem already addressed by Bentham et al. (1993). Modern studies of braided rivers are biased towards regionally degrading and laterally confined fluvial environments with a low preservation potential in the geological record. Consequently, the models based on these studies do not encompass the entire range of ancient braided river environments. Bentham et al. (1993) proposed a new model for braided rivers that accounts for the preservation of thick sequences of overbank fines. Although the model, consisting of four lithofacies, was created to explain the observations made within the Escanilla Formation in Spain, it can be perfectly applied to the Iren Dabasu Formation (Table 5). Facies C1 and F4 (see Table 4 for the codes) of the Iren Dabasu Formation fit the description and the interpretation of the gravel-dominated channel-fill sequences of Bentham et al. (1993). Facies F4, however, is interpreted as an in-channel deposit during a temporary abandonment of the channel due to low water-levels and not as the final stages of an avulsion event. The sand-dominated channel-fill sequences are represented in the Iren Dabasu Formation by Facies C2 and C3. Facies C3 confirms the interpretation of these minor channels as avulsion-related channels. The sheet sandstone splay deposits correspond to Facies F1 as described by Currie and Eberth (1993). In the present study, the pedogenically modified overbank sediments were divided into two categories: Facies F2, massive overbank fines with palaeosol development and the occurrence of bone beds, and Facies F3, thinly bedded clays and silts forming the episodic infill of an abandoned channel. As in the Escanilla Formation, no mature calcretes have been observed in the Iren Dabasu Formation, indicating rapid aggradation of the basin during the Late Cretaceous. The correspondence between the model proposed by Bentham et al. (1993) for the Escanilla Formation and the sedimentary pattern of the Iren Dabasu Formation supports the validity of this model.

According to Leopold and Wolman (1957), braiding occurs by sorting when the stream is temporarily unable to move portions of its load. As a consequence, sorting occurs and the coarser part of the load will form in-channel bars. Considering the palaeogeographical and palaeoclimatic setting, the braided character of the ancient system seems inevitable. During the Cretaceous Period, the region studied was located as far, or further, from the nearest coastline as it is today (Chen, 1987; Smith et al., 1994). Consequently, the prevailing local climate during Cretaceous times had a high degree of continentality. Like the present-day climate, it was characterised by seasonal extremes in temperature and precipitation. The presence of calcretes limits the amount of annual precipitation to 760 mm (Royer, 1999). Under Cretaceous conditions, these palaeoclimatic settings led to a maximal sediment yield (Schumm, 1968). The ancient fluvial environment was characterised by a highly variable discharge and a high sediment yield. Similar conditions give rise to braided rivers in recent fluvial settings (Miall, 1977).

Exposures in the northern part along the dry river valley (ERHVAL) testify to the greatest fluvial activity and represent the ancient major channel with a northward flow. The minor channels, exposed in the southern part, represent more distal (i.e., further from the main channel) braids on the floodplain of the ancient fluvial system. An alternative palaeogeographical model seems possible, whereby the sediments in the northern area represent a northward-flowing main channel, draining the southern area, while the ancillary channels of the southern area, with a flow to the northwest and southwest, join the main channel roughly at right-angles.

Table 5
Comparison of the facies of the braided river model of Bentham et al. (1993) with the Iren Dabasu Formation

Facies (Bentham et al., 1993)	Interpretation (Bentham et al., 1993)	Corresponding facies of the Iren Dabasu Formation
Gravel-dominated channel-fill sequences	Major trunk of braided stream, fining-up trend reflects a phase of channel-system aggradation; fine-grained deposits represent phases of abandonment of the channel	Major channel Type 1 (C1) Fine-grained deposits Type 4 (F4)
Sand-dominated channel-fill sequences	Short-lived, stable splay channels, developed during the later stages of a major trunk-stream avulsion event, that aggrade vertically rather than migrate laterally	Minor channel Type 2 (C2) Minor channel Type 3 (C3)
Sheet sandstone splay deposits	Unconfined tabular splays developed during overbank flooding	Fine-grained deposits Type 1 (F1)
Pedogenically modified overbank sediment	Suspension deposits of largely unconfined sediment-charged flow during times of widespread overbank flooding	Fine-grained deposits Type 2 (F2) Fine-grained deposits Type 3 (F3)

Such an angular river pattern is characteristic of modern foreland basin and basin-margin settings. In modern examples, extensive lakes, ponds, marshes and natural springs, associated with a rich fauna, occur at the confluence of the trunk and ancillary channels. However, considering outcrop patterns and the palaeocurrent measurements, it is difficult to draw such a river pattern without changing the flow direction. Although this second model cannot be excluded, it does not fit the data as well as the first.

6. Conclusions

During Late Cretaceous times, the Iren Nor region was a rapidly aggrading, braided fluvial environment (Fig. 15) with a large floodplain. Fluvial activity in these channels was limited to periods of high discharge within the main channel. The floodplain environments had good vegetative cover, reflected in the palaeosol development and the numerous herbivorous dinosaurs that occur in both the channel and the floodplain sediments. On the floodplain, temporary water-bodies accommodated charophytes and ostracods. Both groups, contrary to the vertebrate data, indicate a latest Cretaceous age (Campanian–Maastrichtian) for the Iren Dabasu Formation. Based on the correlation with the Nemegt Formation, the age estimation can probably be refined to the latest Campanian–Early Maastrichtian.

Acknowledgements

We express our gratitude to all participants in the fieldwork at Erenhot: Feng Lu, Li Wenguo, Li Hong, Guo Dianyong, Shang Changyong, Zhang Zheming, Zhao Xuedong, Dong Yulong, Sun Yan, Tao Xishun, Meng Huanan, Wei Qiang, Liu Hongyuan, Wang Hongjiang, Géraldine Garcia, H. De Potter, J.-J. Blairvacq, P. Godefroit, T. Hubin and T. Smith. Ning Peiji (Director of Erlian Dinosaur Museum) kindly guided us in the Iren Nor region. Shao Qinglong (Inner Mongolia Museum), Monnik Desmeth (Office of Scientific and Cultural Affairs) and Chen Ming (Scientific and Technical Service of the Chinese Embassy in Belgium) handled the financial and administrative part of the excavation campaigns at Erenhot. Ivo Luyckx made the thin-sections and Danny Coetermans did the chemical analyses. Julien Cilis is thanked for the excellent SEM pictures. Jimmy Van Itterbeeck was Research Assistant of the Fund for Scientific Research-Flanders (FWO-Vlaanderen, Belgium) during the course of this study. Thorough reviews by Drs Ian Slipper and David Martill greatly improved the presentation and content of the final manuscript.

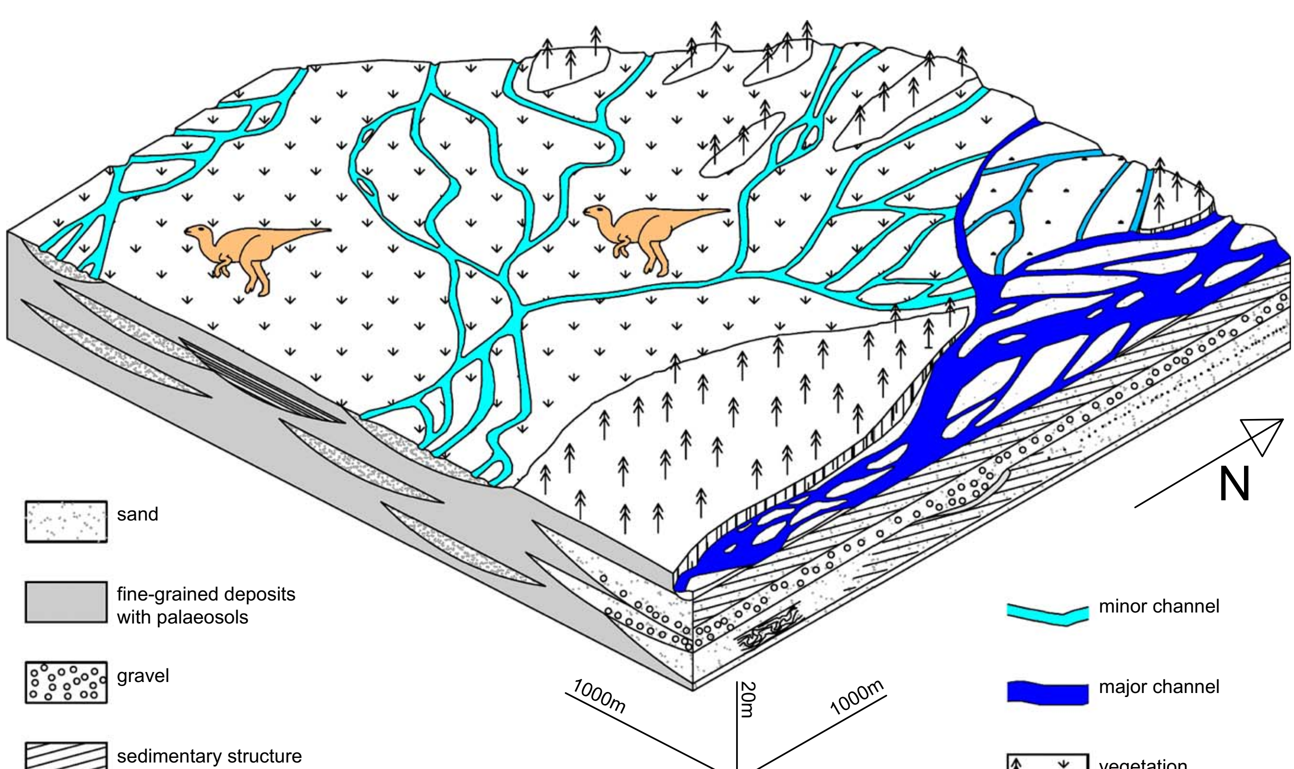

Fig. 15. Three-dimensional model of a braided river valley (based on block diagram of Williams and Rust, 1969) to explain lateral and vertical facies changes within the Iren Dabasu Formation.

References

Barsbold, R., 1972. Biostratigraphy and freshwater molluscs of the Upper Cretaceous of the Gobi part of the Mongolian P.R. Izdatelstvo Nauka, Moscow, 88 pp. (in Russian).

Behrensmeyer, A.K., 1982. Time resolution in fluvial vertebrate assemblages. Paleobiology 8, 211–227.

Behrensmeyer, A.K., 1988. Vertebrate preservation in fluvial channels. Palaeogeography, Palaeoclimatology, Palaeoecology 63, 183–199.

Bentham, P.A., Talling, P.J., Burbank, D.W., 1993. Braided stream and flood-plain deposition in a rapidly aggrading basin: the Escanilla Formation, Spanish Pyrenees. In: Best, J.L., Bristow, C.S. (Eds.), Braided Rivers. Geological Society, London, Special Publication 75, 177–194.

Berkey, C.P., Morris, F.K., 1927. Natural History of Central Asia, Volume II. Geology of Mongolia. The American Museum of Natural History, New York, 475 pp.

Bosquet, J.A.H., 1852. Description des entomostracés fossils des terrains Tertiares de la France et de la Belgique. Académie Royale des Sciences, Lettres et Beaux-Arts de la Belgique, Mémoires 24, 124 pp.

Brett-Surman, M.K., 1979. Phylogeny and palaeobiogeography of hadrosaurian dinosaurs. Nature 277, 560–562.

Bureau of Geology and Mineral Resources of the Nei Mongol Autonomous Region, 1991. Regional geology of the Nei Mongol (Inner Mongolia) Autonomous Region, People's Republic of China. Geological Memoirs, Series 1, 25. Geological Publishing House, Bejing, 725 pp. (in Chinese, English summary).

Chakrabarti, A., 1977. Upward flow and convolute laminations. Senckenbergiana Maritima 9, 285–305.

Chen, P., 1983. A survey of the non-marine Cretaceous of China. Cretaceous Research 4, 123–143.

Chen, P., 1987. Cretaceous paleogeography in China. Palaeogeography, Palaeoclimatology, Palaeoecology 56, 49–56.

Chen, T., 1965. The ostracode genus *Metacypris* and its allies. Acta Palaeontologica Sinica 13, 1–28 (in Chinese, English summary).

Currie, P.J., Eberth, D.A., 1993. Palaeontology, sedimentology and palaeoecology of the Iren Dabasu Formation (Upper Cretaceous), Inner Mongolia, People's Republic of China. Cretaceous Research 14, 127–144.

Eberth, D.A., 1993. Depositional environments and facies transitions of the dinosaur-bearing Upper Cretaceous redbeds at Bayan Mandahu (Inner Mongolia, People's Republic of China). Canadian Journal of Earth Sciences 30, 2196–2213.

Feist, M., Wang, Z., 1995. The species concept in Clavatoraceae (fossil Charophyta) reviewed. Taxon 44, 351–361.

Fox, R.E., 1978. Upper Cretaceous terrestrial vertebrate stratigraphy of the Gobi Desert (Mongolian People's Republic) and western North America. Geological Association of Canada, Special Paper 18, 571–594.

Galeeva, L.I., 1955. Ostracoda from the Cretaceous deposits of the Mongolian People's Republic. Gostoptekhizdat, Moscow, 98 pp. (in Russian).

Gereltsetseg, L., 1998. Mesozoic and Cenozoic charophyta of Mongolia. Mongolian Geoscientist 9, 47.

Gereltsetseg, L., 2001. Mesozoic and Cenozoic charophyta of Mongolia. In: Proceedings of Meeting, ICGP Projects 410 and 421. Mongolian Technical University, School of Geology, Ulan Bataar, pp. 110–112.

Gilmore, C.W., 1933. On the dinosaurian fauna of the Iren Dabasu Formation. Bulletin of the American Museum of Natural History 67, 23–78.

Godefroit, P., Dong, Z., Bultynck, P., Li, H., Feng, L., 1998. New *Bactrosaurus* (Dinosauria: Hadrosauridea) material from Iren Dabasu (Inner Mongolia, P.R. China). Bulletin de l'Institut Royale des Sciences Naturelles de la Belgique – Sciences de la Terre, 68 (Supplement), 3–70.

Gou, Y., Cao, M., 1983. Stratigraphic and biogeographic distribution of the *Cypridea*-bearing faunas in China. In: Maddocks, R.F. (Ed.), Applications of Ostracoda. Proceedings of the Eighth International Symposium on Ostracoda, July 26–29, 1982. University of Houston, Houston, Texas, pp. 381–393.

Gradzinski, R., Jerzykiewicz, T., 1974. Sedimentation of the Barun Goyot Formation. Palaeontologia Polonica 30, 111–146.

Gradzinski, R., Kielan-Jaworowska, Z., Maryanska, T., 1977. Upper Cretaceous Djadokhta, Barun Goyot and Nemegt formations of Mongolia, including remarks on previous subdivisions. Acta Geologica Polonica 27, 281–318.

Graham, S.A., Hendrix, M.S., Johnson, C.L., Badamgarav, D., Badarch, G., Amory, J., Porter, M., Barsbold, R., Webb, L.E., Hacker, B.R., 2001. Sedimentary record and tectonic implications of Mesozoic rifting in southeast Mongolia. Geological Society of America, Bulletin 113, 1560–1579.

Grambast, L., 1962. Classification de l'embranchement des Charophytes. Naturalia Monspeliensia, Série Botanique 14, 63–86.

Grambast-Fessard, N., 1980. Description de deux espèces nouvelles d'*Atopochara* Peck (Clavatoraceae, Charophyta). Geobios 13, 129–135.

Granger, W., Berkey, C.P., 1922. Discovery of Cretaceous and older Tertiary strata in Mongolia. American Museum Novitates 42, 1–7.

Hao, Y., 1988. Cretaceous and Palaeogene ostracod biostratigraphy in Xining and Minhe basins of China. In: Hanai, T., Ikeya, N., Ishizaki, K. (Eds.), Evolutionary Biology of Ostracoda, its Fundamentals and Applications. Elsevier, Tokyo, pp. 1163–1171.

Hao, Y., Su, D., Li, Y., 1983. Late Mesozoic nonmarine ostracods in China. In: Maddocks, R.F. (Ed.), Applications of Ostracoda, Proceedings of the Eighth International Symposium on Ostracoda July 26–29, 1982. University of Houston, Houston, Texas, pp. 372–380.

Hao, Y., Su, D., Li, Y., Ruan, P., Yuan, F., 1974. Cretaceous–Tertiary Ostracoda. Geological Publishing House, Beijing, 94 pp. (in Chinese).

He, J., Yang, H., Yuan, P., 1981. Some ostracods from the Chishan Formation (Upper Cretaceous) of Jurong, southern Jiangsu. Acta Palaeontologica Sinica 20, 341–348 (in Chinese, English summary).

Hicks, J.F., Brinkman, D.L., Nichols, D.J., Watabe, M., 1999. Paleomagnetic and palynologic analyses of Albian to Santonian strata at Bayn Shireh, Burkhant, and Khuren Dukh, eastern Gobi Desert, Mongolia. Cretaceous Research 20, 829–850.

Horne, D.J., Martens, K., 1998. An assessment of the importance of resting eggs for the evolutionary success of Mesozoic non-marine cyrpidoidean Ostracoda (Crustacea). Archiv für Hydrobiologie – Advances in Limnology 52, 549–561.

Hou, Y., Chen, T., Yang, H., Ho, J., Zhou, Q., Tian, M., 1982. Cretaceous–Quaternary ostracode fauna from Jiangsu. Geological Publishing House, Beijing, 298 pp. (in Chinese).

Hou, Y., Gou, Y., Chen, D., 2002. Superfamilies Cypridacea and Darwinulidacea. Fossil Ostracoda of China, vol. 1. Nanjing Institute of Geology and Palaeontology, Academia Sinica, 1090 pp. (in Chinese, English summary).

Huang, R., 1988. Charophytes of Nanxiong Basin, Guangdong and its Cretaceous-Tertiary boundary. Acta Palaeontologica Sinica 27, 457–474 (in Chinese, English summary).

Huang, R., Zhang, J., 1984. Late Cretaceous and Paleogene charophytes from the Sanshui Basin of Guangdong. Bulletin of the Nanjing Institute of Geology and Palaeontology, Academia Sinica 9, 169–210 (in Chinese, English summary).

Huang, R., Zhao, Z., 1989. Charophytes from the Taizhou Formation and the first member of Funing Formation, North Jiangsu Basin in addition to their ages. Bulletin of the Nanjing Institue of Geology and Palaeontology, Academia Sinica 14, 111–127 (in Chinese, English summary).

Jerzykiewicz, T., 1995. Cretaceous vertebrate-bearing strata of the Gobi and Ordos basins – a demise of the Central Asian lacustrine dinosaur habitat. Proceedings of the 15th International Symposium of Kyungpook National University, 1995, 233–256.

Jerzykiewicz, T., Currie, P.J., Eberth, D.A., Johnston, P.A., Koster, E.H., Zheng, J., 1993. Djadokhta Formation correlative strata in Chinese Inner Mongolia: an overview of the stratigraphy, sedimentary geology and, palaeontology and comparisons with the type locality in the pre-Altai Gobi. Canadian Journal of Earth Sciences 30, 2180–2195.

Jerzykiewicz, T., Russell, D.A., 1991. Late Mesozoic stratigraphy and vertebrates of the Gobi Basin. Cretaceous Research 12, 345–377.

Jones, T.R., 1885. On the Ostracoda of the Purbeck Formation, with notes on the Wealden species. Quaterly Journal of the Geological Society of London 61, 311–353.

Karczewska, J., Ziembinska-Tworzydlo, M., 1969. Upper Cretaceous Charophyta from the Nemegt Basin Gobi Desert. Paleontologia Polonica 21, 121–144.

Karczewska, J., Ziembinska-Tworzydlo, M., 1973. Lower Tertiary Charophyta from the Nemegt Basin, Gobi Desert. Palaeontologia Polonica 27, 51–81.

Karczewska, J., Ziembinska-Tworzydlo, M., 1981. New Upper Cretaceous Charophyta from the Nemegt Basin, Gobi Desert. Palaeontologia Polonica 42, 97–146.

Karczewska, J., Ziembinska-Tworzydlo, M., 1983. Age of the Upper Cretaceous Nemegt Formation (Mongolia) on charophytan evidence. Acta Palaeontologica Polonica 28, 137–146.

Khand, Y., 1977. New ostracod species from Upper Cretaceous and Paleogene deposits of Transaltaic Gobi of Mongolia. The Joint Soviet-Mongolian Paleontological Expedition, Transactions 4, 106–111 (in Russian).

Khand, Y., 1987. Late Cretaceous and Early Paleogene ostracods of Mongolia and their stratigraphic significance. Akademia Nauk SSSR, Paleontologicheskii Institut, Moscow, 22 pp. (in Russian).

Khand, Y., 1994. New Upper Cretaceous cypridids (Ostracoda, Cyprididae) of Mongolia. Paleontologicheskii Zhurnal 12, 126–129 (in Russian).

Khand, Y., 2000. The origins of modern nonmarine ostracod faunas: evidence from the Late Cretaceous and Early Palaeogene of Mongolia. Hydrobiologia 419, 119–124.

Krassilov, V., 1982. Early Cretaceous flora of Mongolia. Palaeontographica B 181, 1–43.

Kyansep-Romashkina, N.P., 1975. Some charophytes from the Upper Jurassic and the Cretaceous of Mongolia. The Joint Soviet-Mongolian Paleontological Expedition, Transactions 2, 181–204 (in Russian).

Kyansep-Romashkina, N.P., 1980. The Late Cretaceous charophyte algae from the lacustrine deposits of Mongolia and the Caucasus. In: Martinson, G.G. (Ed.), Limnobios of Ancient Lacustrine Basins of Eurasia. Nauka, Leningrad, pp. 71–90 (in Russian).

Kyansep-Romashkina, N.P., 1982. Distribution of charophyte algae in the Mesozoic lake basins of Mongolia and conditions of their growth. In: Martinson, G.G. (Ed.), Mesozoic Lake Basins of Mongolia. Nauka, Leningrad, pp. 158–193 (in Russian).

Leopold, L.B., Wolman, M.G., 1957. River channel patterns, braided, meandering and straight. United States Geological Survey, Professional Papers 282B, 39–85.

Li, W., Liu, Z., 1994. The Cretaceous palynofloras and their bearing on stratigraphical correlation in China. Cretaceous Research 15, 333–365.

Lillegraven, J.A., McKenna, M.C., 1986. Fossil mammals from the "Mesaverde" Formation (Late Cretaceous, Judithian) of the Bighorn and Wind River Basins, Wyoming, with definitions of Late Cretaceous North American Land-Mammal "Ages". American Museum Novitates 2840, 1–68.

Lin, X., 1989. Cretaceous fossil charophytes in Zhejiang. Geology of Zhejiang 1, 1–11 (in Chinese, English summary).

Liu, J., 1987. Late Cretaceous–Tertiary charophytes from the Shalamulun area of Inner Mongolia. Professional Papers on Stratigraphy and Palaeontology 19, 129–154 (in Chinese, English summary).

Liu, J., Pang, Q., 1999. Charophyte flora from the Late Cretaceous in Tianzhen, Shanxi Province and Yangyuan, Hebei Province. Professional Papers on Stratigraphy and Palaeontology 27, 1–7 (in Chinese, English summary).

Liu, J., Wu, X., 1990. Cretaceous–Tertiary charophyte fossils in northern Xinjiang. In: Study on the Micropaleobotany from the Cretaceous–Tertiary of the Oil-bearing Basins in Some Regions of Qinghai and Xinjiang. China Environment Science Press, pp. 181–229 (in Chinese, English summary).

Liubimova, P.S., 1956. Ostracods from the Cretaceous strata of the eastern part of the Mongolian P.R. Trudy VNIGRI (New Series) 93, 1–174 (in Russian).

Ma, Q., 1994. Nonmarine Cretaceous bivalve assemblages in China. Cretaceous Research 15, 271–284.

Mack, G.H., James, C.W., Monger, C.H., 1993. Classification of paleosols. Geological Society of America, Bulletin 105, 129–136.

Mädler, K., 1955. Die taxionomischen Prinzipien bei der Beurteilung fossiler Charophyten. Paläontologische Zeitschrift 29, 103–108.

Makulekov, N., Kurzanov, S.M., 1986. The biostratigraphical relationships of the Late Cretaceous biota of Mongolia. The Joint Soviet-Mongolian Paleontological Expedition, Transactions 29, 106–112 (in Russian).

Martin-Closas, C., 1996. A phylogenetic system of Clavatoraceae (fossil Charophyta). Review of Palaeobotany and Palynology 94, 259–293.

Martin-Closas, C., Schudack, M.E., 1997. On the concept of species in fossil Charophyta. A reply to Feist and Wang. Taxon 46, 521–525.

Martinson, G.G., 1982. Upper Cretaceous molluscs of Mongolia (systematics, stratigraphy, taphonomy). The Joint Soviet-Mongolian Paleontological Expedition, Transactions 17, 1–83 (in Russian).

Martinson, G.G., Kolesnikov, C.M., 1974. Cretaceous limnetic mollusca from fossiliferous rock tables in Mongolia. The Joint Soviet-Mongolian Paleontological Expedition, Transactions 1, 235–246 (in Russian).

MacNeill, F.S., 1936. In: Morris, F.K. (Ed.), Central Asia in Cretaceous time. Geological Society of America, Bulletin 47, 1477–1534.

McKee, E.D., Crosby, E.J., Berryhill Jr., H.L., 1967. Flood deposits, Bijou Creek, Colorado, June 1965. Journal of Sedimentary Petrology 37, 829–851.

Meng, Q., Hu, J., Jin, J., Zhang, Y., Xu, D., 2003. Tectonics of the late Mesozoic wide extensional basin system in the China-Mongolian border region. Basin Research 15, 397–415.

Miall, A.D., 1977. A review of the braided-river depositional environment. Earth-Science Reviews 13, 1–62.

Miall, A.D., 1996. The Geology of Fluvial Deposits: Sedimentary Facies, Basin Analysis and Petroleum Geology. Springer Verlag, New York, 582 pp.

Nessov, L.A., 1984. Data on late Mesozoic turtles of the U.S.S.R. Studia Palaeocheloniologica 1, 215–223 (in Russian).

Pang, Q., Whatley, R., 1990. The biostratigraphical sequence of Mesozoic non-marine ostracod assemblages in northern China. In: Whatley, R., Maybury, C. (Eds.), Ostracoda and Global Events. Chapman and Hall, London, pp. 239–250.

Pang, Q., Zhang, L., Wang, Q., 1984. Ostracoda. In: Tianjiin Institute of Geology and Mineral Rescources (Eds.), Palaeontological Atlas of North China, Micropalaeontological, vol. III. Geological Publishing House, Beijing, pp. 59–199 (in Chinese).

Peck, R.E., 1937. Morrison Charophyta from Wyoming. Journal of Paleontology 11, 83–90.

Peck, R.E., 1938. A new family of Charophyta from the Lower Cretaceous of Texas. Journal of Paleontology 12, 173–176.

Peck, R.E., 1941. Lower Cretaceous Rocky Mountain nonmarine microfossils. Journal of Paleontology 5, 285–304.

Peck, R.E., 1951. Non-marine ostracods – the subfamily Cyprideinae in the Rocky Mountains area. Journal of Paleontology 25, 307–320.

Peck, R.E., 1957. North American Mesozoic Charophyta. United States Geological Survey, Professional Paper 294A, 1–44.

Reinfelds, I., Nanson, G., 1993. Formation of braided river floodplains, Waimakariri River, New Zealand. Sedimentology 40, 1113–1127.

Royer, D.L., 1999. Depth to pedogenic carbonate horizon as a paleoprecipitation indicator? Geology 27, 1123–1126.

Rozhdestvensky, A.K., 1966. New iguanodonts from Central Asia: phylogenetic and taxonomic relationships between late Iguanodontidae and early Hadrosauridae. Paleontologicheskii Zhurnal 1966, 103–116.

Rozhdestvensky, A.K., 1977. The study of dinosaurs in Asia. Journal of the Palaeontological Society of India 20, 102–119.

Rust, B.R., 1975. Structure and process in a braided river. Sedimentology 18, 221–245.

Schumm, S.A., 1968. Speculations concerning paleohydrologic controls of terrestrial sedimentation. Geological Society of America, Bulletin 79, 1573–1588.

Shajkin, I.M., 1976. New data on biostratigraphy of the Jurassic–Cretaceous deposits of the Fore-Dobrogean Trough. Geologicheskii Zhurnal, Kiev 36, 77–86 (in Russian).

Shuvalov, V.F., 2000. The Cretaceous stratigraphy and palaeobiogeography of Mongolia. In: Benton, M.J., Shishkin, M.A., Unwin, D.M., Kurochkin, E.N. (Eds.), The Age of Dinosaurs in Russia and Mongolia. Cambridge University Press, Cambridge, pp. 256–278.

Smith, A.G., Smith, D.G., Funnell, B.M., 1994. Atlas of Mesozoic and Cenozoic Coastlines. Cambridge University Press, Cambridge, 109 pp.

Stankevitch, E.S., 1982. The late Cretaceous ostracods and their habitat environments. In: Martinson, G.G. (Ed.), Mesozoic Lake Basins of Mongolia. Nauka, Leningrad, pp. 145–157 (in Russian).

Stankevitch, E.S., Sochava, A.V., 1974. Ostracods of the Senonian of Mongolia. The Joint Soviet-Mongolian Paleontological Expedition, Transactions 1, 268–289 (in Russian).

Szczechura, J., 1978. Freshwater ostracods from the Nemegt Formation (Upper Cretaceous) of Mongolia. Palaeontologia Polonica 38, 65–121.

Szczechura, J., Blaszyk, J., 1969. Fresh-water ostracoda from the Upper Cretaceous of the Nemegt Basin, Gobi Desert. Palaeontologia Polonica 21, 107–118.

Tsogbataar, K., 1997. Preliminary study on Mongolian hadrosaurids. In: Mongolia-Japan Joint Paleontological Expedition. Mongolian Paleontological Centre, Ulaan Bataar, 15 pp.

Van Itterbeeck, J., Markevich, V.S., Horne, D.J., 2004. The age of the dinosaur-bearing Cretaceous sediments at Dasuiguo, Inner Mongolia, P.R. China based on charophytes, ostracods and palynomorphs. Cretaceous Research 25, 391–409.

Vasiliev, V.G., Volkhonin, V.C., Grishin, G.L., Ivanov, A.K., Marinov, I.A., Mokshancev, K.B., 1959. Geological structure of the People's Republic of Mongolia (stratigraphy and tectonics). Gostoptekhizdat, Leningrad, 492 pp. (in Russian).

Vavra, W., 1891. Monographie der Ostracoden Böhmens. Archiv der Naturwissenschaftlichen Landesdurchforschung von Böhmen 8 (3), 1–116.

Wang, Z., 1978. Cretaceous charophytes from the Yangtze-Han river basin with a note on the classification of Porocharaceae and Characeae. Memoirs of the Nanjing Institute of Geology and Palaeontology, Academia Sinica 9, 61–88 (in Chinese, English summary).

Wang, Z., Huang, R., Wang, S., 1976. Mesozoic and Cenozoic charophyta from Yunnan Province. In: Nanjing Geological and Paleobotanical Institute, Academia Sinica (Ed.), Mesozoic fossils of Yunnan. Science Press, Beijing, pp. 65–86 (in Chinese).

Wang, Z., Lu, H., Zhao, C., 1985. Cretaceous charophytes from Songliao Basin and adjacent areas. Tectonic and Scientific Press of Heilongjiang, Harbin, 75 pp. (in Chinese, English summary).

Wang, Z., Yuan, P., Zhao, Z., 1983. Chihshan Formation and fossil charophytes. Acta Palaeontologica Sinica 22, 493–504 (in Chinese, English summary).

Weishampel, D.B., 1990. Dinosaur distribution. In: Weishampel, D.B., Dodson, P., Osmolska, H. (Eds.), The Dinosauria. University of California Press, Los Angeles, pp. 63–139.

Weishampel, D.B., Horner, J.R., 1986. The hadrosaurid dinosaurs of the Iren Dabasu Formation (People's Republic of China, Late Cretaceous). Journal of Vertebrate Paleontology 6, 38–45.

Williams, P.F., Rust, B.R., 1969. The sedimentology of a braided river. Journal of Sedimentary Petrology 39, 649–679.

Ye, C., 1994. Succession of Cypridacea (Ostracoda) and nonmarine Cretaceous stratigraphy of China. Cretaceous Research 15, 285–303.

Ye, D., 1990. The geological and exploration significance of Cretaceous nonmarine ostracoda from the Hailaer Basin, northwestern China. In: Whatley, R., Maybury, C. (Eds.), Ostracoda and Global Events. Chapman and Hall, London, pp. 251–261.

Zhang, Y., Li, J., 2000. Cretaceous palynofloral succession of the Jiangsu area. Journal of Stratigraphy 24, 65–71.